Cancer Cell
Minireview

NKX2-1/TTF-1: An Enigmatic Oncogene that Functions as a Double-Edged Sword for Cancer Cell Survival and Progression

Tomoya Yamaguchi,[1] Yasuyuki Hosono,[1] Kiyoshi Yanagisawa,[1] and Takashi Takahashi[1,*]
[1]Division of Molecular Carcinogenesis, Center for Neurological Diseases and Cancer, Nagoya University Graduate School of Medicine, Nagoya 466-8550, Japan
*Correspondence: tak@med.nagoya-u.ac.jp
http://dx.doi.org/10.1016/j.ccr.2013.04.002

Emerging evidence indicates that NKX2-1, a homeobox-containing transcription factor also known as TTF-1, plays a role as a "lineage-survival" oncogene in lung adenocarcinomas. In T cell acute lymphoblastic leukemia, gene rearrangements lead to aberrant expression of NKX2-1/TTF-1. Despite accumulating evidence supporting its oncogenic role, it has become apparent that NKX2-1/TTF-1 expression also has biological and clinical functions in the opposite direction that act against tumor progression. Herein, we review recent findings showing these enigmatic double-edged characteristics, with special attention given to the roles of NKX2-1/TTF-1 in lung development and carcinogenesis.

Oncogenic Involvement of NKX2-1/TTF-1

Emerging evidence suggests that "lineage-specific addiction" to survival mechanisms that are programmed for developmental roles in normal progenitor cells of particular lineages may exist in cancer cells. The transcription factor MITF in melanoma is considered to be an archetypal prototype (Garraway and Sellers, 2006), whereas survival of lung cancers with neuroendocrine (NE) features such as small-cell lung cancer (SCLC) is dependent on continued expression of ASH1, a transcription factor indispensable for pulmonary NE cell development (Nishikawa et al., 2011; Osada et al., 2005, 2008). Thyroid transcription factor 1 (TTF-1), also known as NKX2-1, is a homeobox-containing transcription factor essential for the development of the lung and thyroid as well as a restricted part of the brain (Stanfel et al., 2005), and a series of peripheral lung cells defined as the terminal respiratory unit (TRU) is under the control of this master regulator. About 70% of adenocarcinomas express NKX2-1/TTF-1 independent of disease stage and retain features of the TRU to a certain extent (Yatabe et al., 2002). These TRU-type adenocarcinomas exhibit a distinctively higher prevalence of *EGFR* mutations, disproportionately high occurrence in females and nonsmokers, and characteristic expression profiles; in fact, *p53* and *KRAS* mutations are inversely associated with NKX2-1/TTF-1 expression (Takeuchi et al., 2006; Yatabe et al., 2005). We and others have previously found that NKX2-1/TTF-1-positive lung adenocarcinomas are dependent on sustained expression of NKX2-1/TTF-1 and sometimes even exhibit focal copy-number increases (Figure 1; Table 1) (Kendall et al., 2007; Kwei et al., 2008; Tanaka et al., 2007; Weir et al., 2007). Intriguingly, *Nkx2-1/Ttf-1* transgenic mice exhibit hyperplasia of type II alveolar cells (Wert et al., 2002). In addition, NKX2-1/TTF-1 is prominently expressed in lung epithelial cells undergoing regeneration (Stahlman et al., 1996). Furthermore, haploinsufficiency of *Nkx2-1/Ttf-1* was recently reported to reduce tumor formation in transgenic mice expressing mutant EGFR (Maeda et al., 2012).

Several lines of evidence suggest possible oncogenic involvement of *NKX2-1/TTF-1* in other types of cancers. In addition to the lung, the thyroid is another organ that expresses NKX2-1/TTF-1. A germline missense mutation of *NKX2-1/TTF-1* that results in a valine substitution for alanine at codon 339 has been identified in families affected by multinodular goiter and papillary thyroid carcinoma (Ngan et al., 2009). It is of note that the SNP rs944289, which maps close to *NKX2-1/TTF-1*, was shown to be significantly associated with increased risk of thyroid cancer (Gudmundsson et al., 2009), although the mechanistic link remains to be elucidated. Rearrangements of *NKX2-1/TTF-1* with T cell receptor or immunoglobulin heavy-chain loci were recently identified in T cell acute lymphoblastic leukemia (T-ALL), suggesting a role in the pathogenesis of hematopoietic malignancies (Homminga et al., 2011). Rearrangements and ectopic expression of *NKX2-2* and *NKX2-5*, both homeobox-containing transcription factors closely related to *NKX2-1/TTF-1*, have also been reported in a subset of T-ALL (Homminga et al., 2011; Nagel et al., 2003). These data strongly suggest an oncogenic role for NKX2-1/TTF-1 as well as other members of the NK2 family, not only in lung and thyroid cancers but also in hematopoietic malignancies. On the other hand, *NKX2-8*, residing in close proximity to *NKX2-1*, exhibits loss of heterozygosity and reduced expression in lung squamous cell carcinomas (Harris et al., 2011), suggesting distinct modes of involvement.

Enigma Surrounding NKX2-1/TTF-1 in Tumor Biology

Despite its role as a lineage-survival oncogene in lung adenocarcinomas, NKX2-1/TTF-1 expression is also known to be associated with favorable prognosis in affected patients (Anagnostou et al., 2009). Evidence to explain this paradox has recently emerged (Figure 2). For example, we found that *MYBPH* is directly transactivated by NKX2-1/TTF-1 and inhibits phosphorylation of the myosin regulatory light chain via direct interaction with ROCK1, which is a prerequisite process for acquisition of assembly competence (Hosono et al., 2012b). In addition, MYBPH directly binds to and inhibits assembly of nonmuscle myosin heavy chain IIA (Hosono et al., 2012a), thereby conferring

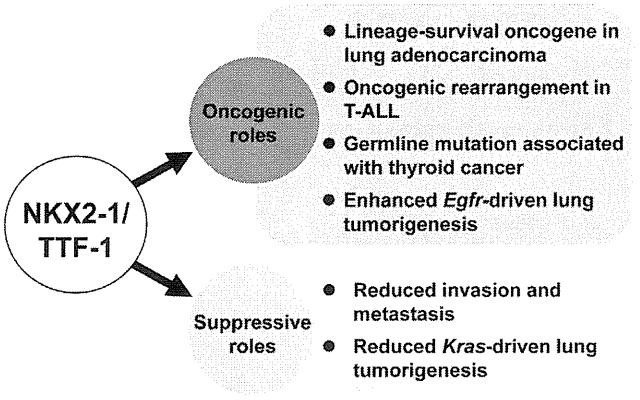

Figure 1. Double-Edged Characteristic of NKX2-1/TTF-1
NKX2-1/TTF-1 has shown both oncogenic and inhibitory activities in cancer development and progression.

firm inhibition of actomyosin assembly by two distinct mechanisms and consequently reducing cell motility, invasion, and metastasis. These apparently deleterious effects in lung adenocarcinoma progression appear to be negated by frequent promoter DNA methylation of *MYBPH*. The epithelial tight-junction protein OCLN as well as two other epithelial tight-junction proteins, CLDN1 and CLDN18, were also shown to be transcriptionally activated by NKX2-1/TTF-1 (Niimi et al., 2001; Runkle et al., 2012). These findings indicate that genes implicated in regulation of cytoskeletal and cell-cell organization are prime transcriptional targets of TTF-1, which negatively affects cell motility, invasion, and metastasis and is also conceivably involved in lung morphogenesis and regeneration after lung injury. In addition, downregulation of *Nkx2-1/Ttf-1* has been shown to lead to eventual derepression of *Hmga2* and acquisition of metastatic ability in a mouse model of lung adenocarcinoma with conditionally activated *Kras* and loss-of-function *p53* mutant alleles (Snyder et al., 2013; Winslow et al., 2011). Interestingly, haploinsufficiency or conditional knockout of *Nkx2-1/Ttf-1* was recently reported to enhance development of invasive *Kras*-driven mucinous lung adenocarcinoma (Maeda et al., 2012; Snyder et al., 2013), in contrast to suppressing *Egfr*-driven lung tumorigenesis (Maeda et al., 2012). Loss of Nkx2-1/Ttf-1 appears to induce the mucin-producing phenotype through consequential release of Foxa1/Foxa2, transcription factors known to physically interact and cooperate with Nkx2-1/Ttf-1, onto de novo binding sites near gastrointestinal differentiation-related genes including Hnf4α, which critically regulates the differentiation program (Snyder et al., 2013). Along this line, it is notable that human invasive mucinous adenocarcinomas of the lung almost invariably express HNF4α, and have exhibited a significant association with negative TTF-1 expression and positive KRAS mutation status (Kunii et al., 2011). Although epithelial-to-mesenchymal transition (EMT) is linked with cancer progression, NKX2-1/TTF-1 represses TGF-β-induced EMT by alleviating TGF-β-mediated induction of Snail and Slug, as well as by reducing TGF-β production (Saito et al., 2009). Conversely, TGF-β represses NKX2-1/TTF-1 by induction of miR-365 (Qi et al., 2012). Thus, accumulated evidence points to the notion that NKX2-1/TTF-1 plays a double-edged role in cancer.

NKX2-1/TTF-1-Mediated Lineage-Survival Signaling

Despite the requirement for sustained NKX2-1/TTF-1 expression in the survival of lung adenocarcinoma cells, NKX2-1/TTF-1 itself cannot be considered as a molecular target for treating this devastating cancer because of its indispensable roles in normal lung physiology, such as the production and secretion of surfactant proteins. Thus, elucidation of how NKX2-1/TTF-1 mediates survival signals has long been anticipated. In this regard, we recently found that NKX2-1/TTF-1 directly transactivates the receptor tyrosine kinase *ROR1*, which in turn sustains a favorable balance between prosurvival PI3K-AKT and proapoptotic p38 signaling, in part through ROR1 kinase-dependent c-Src activation as well as kinase activity-independent sustainment of EGFR-ERBB3 association, ERBB3 phosphorylation, and consequential PI3K activation (Yamaguchi et al., 2012). These findings may underlie the molecular basis for the functional interrelationship between NKX2-1/TTF-1 and EGFR. Consistently, NKX2-1/TTF-1 expression is significantly associated with *EGFR* mutations in lung cancer tissues (Takeuchi et al., 2006; Yatabe et al., 2005), and *Nkx2-1/Ttf-1* haploinsufficiency reduces mutant *Egfr*-driven lung tumorigenesis (Maeda et al., 2012). It is also of particular interest from a clinical point of view that ROR1 inhibition appears to be effective for treatment of lung adenocarcinomas carrying various gefitinib-resistance mechanisms, such as secondary EGFR mutations and HGF overexpression, because the existence of such diverse mechanisms makes it difficult to predict which should be targeted to prevent expansion of resistant clones. This molecule with possible druggability, namely a cell-surface receptor with a

Table 1. Alterations of the NK2 Family in Human Cancers

NK2 Family	Aberrations	Organ Sites	Cancer Types	References
NKX2-1	amplification	lung	adenocarcinoma	Tanaka et al., 2007
	amplification	lung	adenocarcinoma	Kendall et al., 2007
	amplification	lung	adenocarcinoma	Weir et al., 2007
	amplification	lung	adenocarcinoma	Kwei et al., 2008
	germline mutation	thyroid	multinodular goiter, papillary adenocarcinoma	Ngan et al., 2009
	rearrangement	hematopoietic	T cell acute lymphoblastic leukemia	Homminga et al., 2011
NKX2-2	rearrangement	hematopoietic	T cell acute lymphoblastic leukemia	Homminga et al., 2011
NKX2-5	rearrangement	hematopoietic	T cell acute lymphoblastic leukemia	Nagel et al., 2003
NKX2-8	loss of heterozygosity	lung	squamous cell carcinoma	Harris et al., 2011

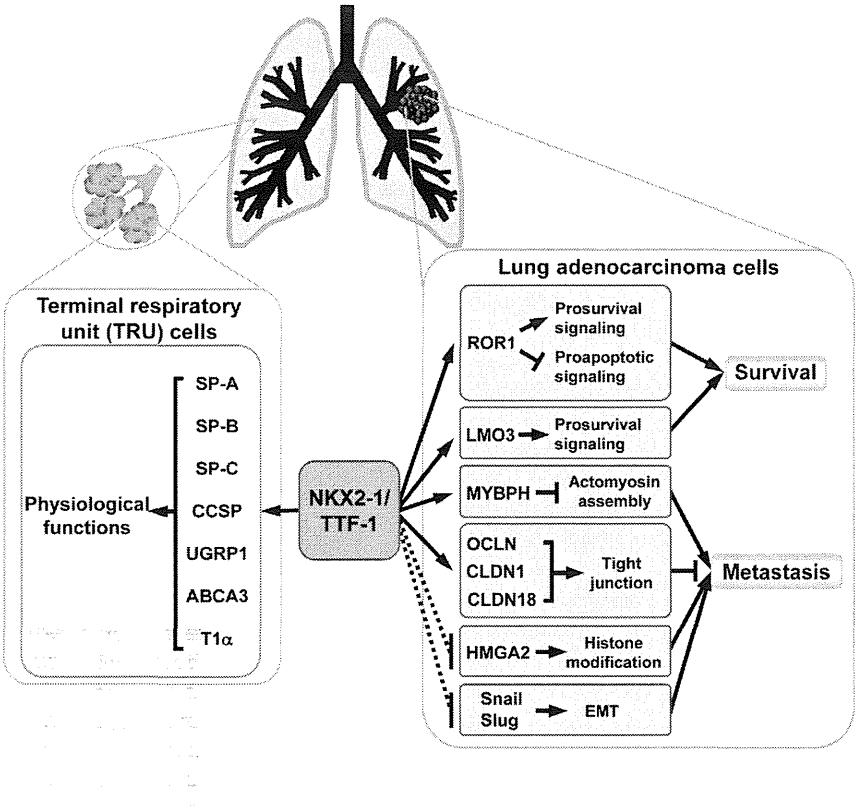

Figure 2. NKX2-1/TTF-1-Mediated Transcriptional Regulation and Consequences in Normal and Cancer Cells of the Lung

NKX2-1/TTF-1 is required for maintenance of physiological lung functions in addition to its developmental roles. The oncogene plays a role as a lineage-survival oncogene in lung adenocarcinomas, whereas it also inhibits invasion, metastasis, and progression, paradoxically conferring better prognosis. Solid and dashed lines represent direct and indirect regulation, respectively.

tyrosine kinase domain, may thus be considered to be an "Achilles' heel" in lung adenocarcinomas, and future development of therapeutic means is greatly anticipated to reduce the intolerable death toll from currently "hard-to-cure" lung adenocarcinomas. In addition to *ROR1*, *LMO3*, a paralog of the *LMO1* and *LMO2* oncogenes in T-ALL, was recently identified as an additional direct transcriptional target for mediating survival signals (Watanabe et al., 2013). NKX2-1/TTF-1 appears to cooperatively transactivate *LMO3* together with FOXA1, whereas *LMO3* knockdown induced apoptosis in a lung adenocarcinoma cell line. However, ectopic overexpression of *LMO3* failed to overcome *NKX2-1/TTF-1* knockdown-induced apoptosis, suggesting the existence of additional crucial targets for lineage-survival signaling in lung adenocarcinoma cells.

Developmental Roles of NKX2-1/TTF-1 in Relation to Cancer Biology

During embryonic lung development, temporal-spatial expression of NKX2-1/TTF-1 is tightly regulated. NKX2-1/TTF-1 expression is first detected in the ventral foregut endoderm during a very early stage and then becomes abundantly expressed in virtually all cells in the progenitor of the trachea arising from the lung primordium. As subsequent branching morphogenesis proceeds, NKX2-1/TTF-1 expression is progressively restricted to distal airway cells and finally confined to epithelial cells in the TRU (Stahlman et al., 1996; Yatabe et al., 2002). A lung rudiment in *Nkx2-1/Ttf-1* knockout mice exhibited proximal, albeit abnormal, airway characteristics, suggesting its dispensable nature in specification of the lung primordium and proximal lung morphogenesis (Minoo et al., 1999). In contrast, this oncogene was shown to be strictly required for distal lung morphogenesis (Yuan et al., 2000). *NKX2-1/TTF-1* critically translates instructive morphogenic signals from the surrounding mesenchyme into transcriptional regulation of its targets, which are mediated by factors including fibroblast growth factors, Sonic hedgehog, and bone morphogenetic proteins. In humans, *NKX2-1/TTF-1* haploinsufficiency confers the rare autosomal-dominant disorder benign hereditary chorea as well as brain-lung-thyroid syndrome, which is manifested by chorea, hypothyroidism, and infantile respiratory distress (Inzelberg et al., 2011). Human *NKX2-1/TTF-1* haploinsufficiency might be associated with lung tumorigenesis in context-dependent and subtype-specific manners, as reported in mice (Maeda et al., 2012; Snyder et al., 2013). Unfortunately, no comprehensive epidemiologic data on the predisposition to lung cancers in affected individuals have been presented.

In addition to lung adenocarcinoma, it is interesting to note that NKX2-1/TTF-1 is frequently detected in SCLCs, which usually arise in the proximal airway, a region that normally lacks NKX2-1/TTF-1 expression. Because NKX2-1/TTF-1 expression is seen in the lung primordium, this phenomenon may reflect an atavistic, yet committed, state of SCLCs, which is consistent with its lack of expression in small-cell carcinomas arising from other organs, despite the similar characteristics of small and round morphology and NE properties. Future study comparing NKX2-1/TTF-1 target gene regulation between adenocarcinomas and those in small-cell carcinomas of various organs, including the adult and developing fetal lungs, would likely shed light on both similarities and distinctions with regard to its functional roles.

Regulation of NKX2-1/TTF-1 and Context Dependence

The 42 kD major isoform is encoded by mRNAs harboring exons 2 and 3, whereas the 44 kD minor isoform is encoded by all three exons (Figure 3). The proximal major promoter contains a TATA-like element and binding sites for FOXA1 (also known as HNF-3α), FOXA2 (HNF-3β), and GATA6, all of which are known to be crucially involved in lung development (Costa et al., 2001). The minor distal promoter is regulated by SP1 and SP3. NKX2-1/TTF-1 directly transactivates multiple genes implicated to have physiological lung functions, including SP-A, SP-B, SP-C, CCSP (also known as CC10, uteroglobin, or secretoglobin),

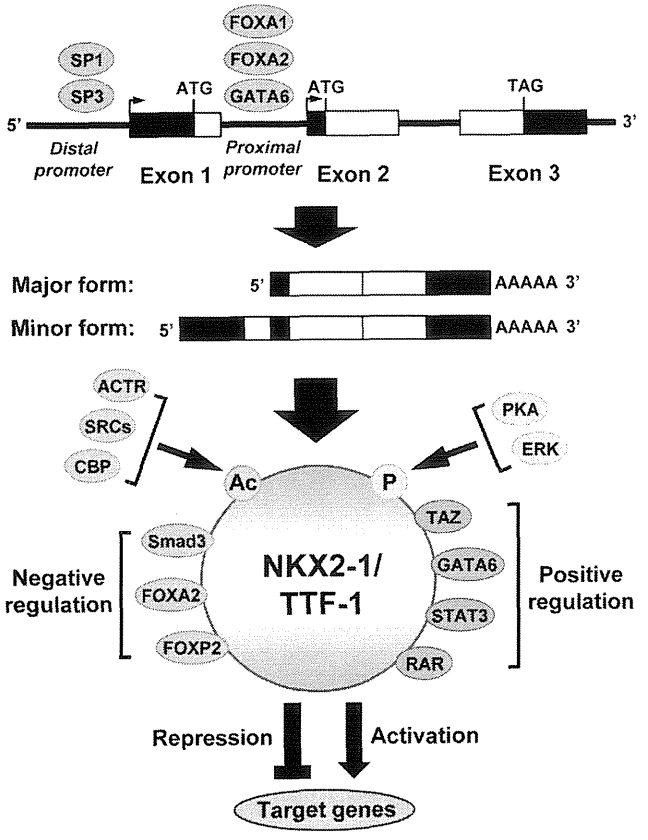

Figure 3. Regulatory Mechanisms of NKX2-1/TTF-1
NKX2-1/TTF-1 is transcribed from two distinct promoters under the influence of various transcription factors. Its transcriptional regulatory activities are modulated in a context-dependent manner, possibly by cooperating transcription factors as well as protein modifications. Ac, acetylation; P, phosphorylation.

UGRP1, and ABCA3. NKX2-1/TTF-1 also transactivates the functions of HOP, an HDAC-dependent negative regulator of NKX2-1/TTF-1 (Yin et al., 2006), as well as T1α, a type I pneumocyte-specific marker (Ramirez et al., 1997). CLDN18 and OCLN tight-junction proteins MYBPH, LMO3, and ROR1 have recently been identified as targets for their roles in cancer, as discussed above. Transcription factors that interact and cooperate with NKX2-1/TTF-1 include FOXA2 (Minoo et al., 2007), FOXP2 (Zhou et al., 2008), GATA6 (Liu et al., 2002), STAT3 (Yan et al., 2002), and RAR (Yan et al., 2001). Furthermore, Smad3 and TAZ modulate the transcriptional activity of NKX2-1/TTF-1 via their binding in a negative and positive manner, respectively (Li et al., 2002; Park et al., 2004). Posttranslational modifications are also important as a regulatory mechanism of NKX2-1/TTF-1 functions. Multiple nuclear coactivators, including ACTR, p160 steroid receptor coactivators, and p300/CBP, acetylate NKX2-1/TTF-1 (Yang et al., 2004), whereas NKX2-1/TTF-1 is also regulated through its phosphorylation, positively by PKA (Yan and Whitsett, 1997) and negatively by ERK (Missero et al., 2000). In addition, Smad3 physically interacts with NKX2-1/TTF-1 and inhibits NKX2-1/TTF-1-mediated transcription from the *SP-B* promoter lacking a Smad binding site (Li et al., 2002).

Recent ChIP-seq and ChIP-chip analyses have revealed a large number of additional potential transcriptional targets of NKX2-1/TTF-1 (Maeda et al., 2012; Tagne et al., 2012; Watanabe et al., 2013), with experimental validation of the induction of LMO3, E2F3, and cyclins B1 and B2, as well as repression of MUC5A, FGFR1, and MET. It is notable that NKX2-1/TTF-1 appears to be associated with and affect promoters via not only its canonical binding sites but also by the AP-1, forkhead, and nuclear hormone receptor-binding motifs. Therefore, downstream targets appear to be regulated by NKX2-1/TTF-1 in a context-dependent manner, possibly reflecting the expression of its cofactors.

Accumulating evidence, as noted above, implicates opposing roles of NKX2-1/TTF-1 in lung cancer development, which may also be the case in thyroid tumors and hematopoietic malignancies. NKX2-1/TTF-1 expression is absolutely required for peripheral lung development and differentiation, whereas its level in lung adenocarcinoma is associated with but not deterministic of differentiated morphologies (Takeuchi et al., 2006; Yatabe et al., 2002). It would be interesting to investigate whether any similarities and/or distinctions exist in the regulation of downstream targets by this enigmatic oncogene in cancer cells as well as in normal development, with special attention given to context dependence.

Conclusions and Future Perspectives

NKX2-1/TTF-1 has long been a focus of research in the field of lung and thyroid physiology, whereas emerging evidence has called attention to its roles in cancer. This oncogene appears to function as a double-edged sword in the pathogenesis of lung adenocarcinoma and possibly in other tumors as well. A future rigorous search for additional downstream molecules is warranted to gain a more complete picture of NKX2-1/TTF-1-centered regulatory networks in order to take advantage of its Jekyll-and-Hyde characteristics. It should also be kept in mind that current understanding of the regulatory web surrounding this enigmatic transcription factor may be oversimplified, as the same architecture may not exist in normal and cancerous states, or even among individual tumors. For example, a sizable fraction of NKX2-1/TTF-1-positive human lung adenocarcinomas are negative for surfactant proteins, which are authentic targets for transcriptional activation in normal lungs, and/or positive for HMGA2, a target for transcriptional repression. Opposing effects of *Nkx2-1/Ttf-1* haploinsufficiency in transgenic mice carrying mutant *Kras* and *Egfr* also suggest its multifaceted nature. Thus, the NKX2-1/TTF-1 regulatory networks present in cells in both normal and cancerous conditions may well be quite complex and context dependent, and likely require a radically different approach to elucidate. Along this line, a cancer systems biology approach with the aid of ever-increasing computing power may help to reveal a path to resolve this challenge, ultimately allowing an opportunity to take advantage of the double-edged characteristics of NKX2-1/TTF-1 in patients affected by cancer.

ACKNOWLEDGMENTS

We thank all of the members of our research group for their invaluable contributions, including helpful discussions and critical comments. We also

apologize for the incompleteness of the referencing due to space constraints. Studies in our laboratory have been supported in part by grants from the Ministry of Education, Science, Sports and Culture, Japan, and the Ministry of Health, Labor and Welfare, Japan.

REFERENCES

Anagnostou, V.K., Syrigos, K.N., Bepler, G., Homer, R.J., and Rimm, D.L. (2009). Thyroid transcription factor 1 is an independent prognostic factor for patients with stage I lung adenocarcinoma. J. Clin. Oncol. *27*, 271–278.

Costa, R.H., Kalinichenko, V.V., and Lim, L. (2001). Transcription factors in mouse lung development and function. Am. J. Physiol. Lung Cell. Mol. Physiol. *280*, L823–L838.

Garraway, L.A., and Sellers, W.R. (2006). Lineage dependency and lineage-survival oncogenes in human cancer. Nat. Rev. Cancer *6*, 593–602.

Gudmundsson, J., Sulem, P., Gudbjartsson, D.F., Jonasson, J.G., Sigurdsson, A., Bergthorsson, J.T., He, H., Blondal, T., Geller, F., Jakobsdottir, M., et al. (2009). Common variants on 9q22.33 and 14q13.3 predispose to thyroid cancer in European populations. Nat. Genet. *41*, 460–464.

Harris, T., Pan, Q., Sironi, J., Lutz, D., Tian, J., Sapkar, J., Perez-Soler, R., Keller, S., and Locker, J. (2011). Both gene amplification and allelic loss occur at 14q13.3 in lung cancer. Clin. Cancer Res. *17*, 690–699.

Homminga, I., Pieters, R., Langerak, A.W., de Rooi, J.J., Stubbs, A., Verstegen, M., Vuerhard, M., Buijs-Gladdines, J., Kooi, C., Klous, P., et al. (2011). Integrated transcript and genome analyses reveal NKX2-1 and MEF2C as potential oncogenes in T cell acute lymphoblastic leukemia. Cancer Cell *19*, 484–497.

Hosono, Y., Usukura, J., Yamaguchi, T., Yanagisawa, K., Suzuki, M., and Takahashi, T. (2012a). MYBPH inhibits NM IIA assembly via direct interaction with NMHC IIA and reduces cell motility. Biochem. Biophys. Res. Commun. *428*, 173–178.

Hosono, Y., Yamaguchi, T., Mizutani, E., Yanagisawa, K., Arima, C., Tomida, S., Shimada, Y., Hiraoka, M., Kato, S., Yokoi, K., et al. (2012b). MYBPH, a transcriptional target of TTF-1, inhibits ROCK1, and reduces cell motility and metastasis. EMBO J. *31*, 481–493.

Inzelberg, R., Weinberger, M., and Gak, E. (2011). Benign hereditary chorea: an update. Parkinsonism Relat. Disord. *17*, 301–307.

Kendall, J., Liu, Q., Bakleh, A., Krasnitz, A., Nguyen, K.C., Lakshmi, B., Gerald, W.L., Powers, S., and Mu, D. (2007). Oncogenic cooperation and coamplification of developmental transcription factor genes in lung cancer. Proc. Natl. Acad. Sci. USA *104*, 16663–16668.

Kunii, R., Jiang, S., Hasegawa, G., Yamamoto, T., Umezu, H., Watanabe, T., Tsuchida, M., Hashimoto, T., Hamakubo, T., Kodama, T., et al. (2011). The predominant expression of hepatocyte nuclear factor 4α (HNF4α) in thyroid transcription factor-1 (TTF-1)-negative pulmonary adenocarcinoma. Histopathology *58*, 467–476.

Kwei, K.A., Kim, Y.H., Girard, L., Kao, J., Pacyna-Gengelbach, M., Salari, K., Lee, J., Choi, Y.L., Sato, M., Wang, P., et al. (2008). Genomic profiling identifies TITF1 as a lineage-specific oncogene amplified in lung cancer. Oncogene *27*, 3635–3640.

Li, C., Zhu, N.L., Tan, R.C., Ballard, P.L., Derynck, R., and Minoo, P. (2002). Transforming growth factor-β inhibits pulmonary surfactant protein B gene transcription through SMAD3 interactions with NKX2.1 and HNF-3 transcription factors. J. Biol. Chem. *277*, 38399–38408.

Liu, C., Glasser, S.W., Wan, H., and Whitsett, J.A. (2002). GATA-6 and thyroid transcription factor-1 directly interact and regulate surfactant protein-C gene expression. J. Biol. Chem. *277*, 4519–4525.

Maeda, Y., Tsuchiya, T., Hao, H., Tompkins, D.H., Xu, Y., Mucenski, M.L., Du, L., Keiser, A.R., Fukazawa, T., Naomoto, Y., et al. (2012). Kras(G12D) and Nkx2-1 haploinsufficiency induce mucinous adenocarcinoma of the lung. J. Clin. Invest. *122*, 4388–4400.

Minoo, P., Su, G., Drum, H., Bringas, P., and Kimura, S. (1999). Defects in tracheoesophageal and lung morphogenesis in Nkx2.1(−/−) mouse embryos. Dev. Biol. *209*, 60–71.

Minoo, P., Hu, L., Xing, Y., Zhu, N.L., Chen, H., Li, M., Borok, Z., and Li, C. (2007). Physical and functional interactions between homeodomain NKX2.1 and winged helix/forkhead FOXA1 in lung epithelial cells. Mol. Cell. Biol. *27*, 2155–2165.

Missero, C., Pirro, M.T., and Di Lauro, R. (2000). Multiple Ras downstream pathways mediate functional repression of the homeobox gene product TTF-1. Mol. Cell. Biol. *20*, 2783–2793.

Nagel, S., Kaufmann, M., Drexler, H.G., and MacLeod, R.A. (2003). The cardiac homeobox gene NKX2-5 is deregulated by juxtaposition with BCL11B in pediatric T-ALL cell lines via a novel t(5;14)(q35.1;q32.2). Cancer Res. *63*, 5329–5334.

Ngan, E.S., Lang, B.H., Liu, T., Shum, C.K., So, M.T., Lau, D.K., Leon, T.Y., Cherny, S.S., Tsai, S.Y., Lo, C.Y., et al. (2009). A germline mutation (A339V) in thyroid transcription factor-1 (TITF-1/NKX2.1) in patients with multinodular goiter and papillary thyroid carcinoma. J. Natl. Cancer Inst. *101*, 162–175.

Niimi, T., Nagashima, K., Ward, J.M., Minoo, P., Zimonjic, D.B., Popescu, N.C., and Kimura, S. (2001). claudin-18, a novel downstream target gene for the T/EBP/NKX2.1 homeodomain transcription factor, encodes lung- and stomach-specific isoforms through alternative splicing. Mol. Cell. Biol. *21*, 7380–7390.

Nishikawa, E., Osada, H., Okazaki, Y., Arima, C., Tomida, S., Tatematsu, Y., Taguchi, A., Shimada, Y., Yanagisawa, K., Yatabe, Y., et al. (2011). miR-375 is activated by ASH1 and inhibits YAP1 in a lineage-dependent manner in lung cancer. Cancer Res. *71*, 6165–6173.

Osada, H., Tatematsu, Y., Yatabe, Y., Horio, Y., and Takahashi, T. (2005). ASH1 gene is a specific therapeutic target for lung cancers with neuroendocrine features. Cancer Res. *65*, 10680–10685.

Osada, H., Tomida, S., Yatabe, Y., Tatematsu, Y., Takeuchi, T., Murakami, H., Kondo, Y., Sekido, Y., and Takahashi, T. (2008). Roles of achaete-scute homologue 1 in DKK1 and E-cadherin repression and neuroendocrine differentiation in lung cancer. Cancer Res. *68*, 1647–1655.

Park, K.S., Whitsett, J.A., Di Palma, T., Hong, J.H., Yaffe, M.B., and Zannini, M. (2004). TAZ interacts with TTF-1 and regulates expression of surfactant protein-C. J. Biol. Chem. *279*, 17384–17390.

Qi, J., Rice, S.J., Salzberg, A.C., Runkle, E.A., Liao, J., Zander, D.S., and Mu, D. (2012). MiR-365 regulates lung cancer and developmental gene thyroid transcription factor 1. Cell Cycle *11*, 177–186.

Ramirez, M.I., Rishi, A.K., Cao, Y.X., and Williams, M.C. (1997). TGT3, thyroid transcription factor I, and Sp1 elements regulate transcriptional activity of the 1.3-kilobase pair promoter of T1α, a lung alveolar type I cell gene. J. Biol. Chem. *272*, 26285–26294.

Runkle, E.A., Rice, S.J., Qi, J., Masser, D., Antonetti, D.A., Winslow, M.M., and Mu, D. (2012). Occludin is a direct target of thyroid transcription factor-1 (TTF-1/NKX2-1). J. Biol. Chem. *287*, 28790–28801.

Saito, R.A., Watabe, T., Horiguchi, K., Kohyama, T., Saitoh, M., Nagase, T., and Miyazono, K. (2009). Thyroid transcription factor-1 inhibits transforming growth factor-β-mediated epithelial-to-mesenchymal transition in lung adenocarcinoma cells. Cancer Res. *69*, 2783–2791.

Snyder, E.L., Watanabe, H., Magendantz, M., Hoersch, S., Chen, T.A., Wang, D.G., Crowley, D., Whittaker, C.A., Meyerson, M., Kimura, S., and Jacks, T. (2013). Nkx2-1 represses a latent gastric differentiation program in lung adenocarcinoma. Mol. Cell. Published online March 19, 2013. http://dx.doi.org/10.1016/j.molcel.2013.02.018.

Stahlman, M.T., Gray, M.E., and Whitsett, J.A. (1996). Expression of thyroid transcription factor-1 (TTF-1) in fetal and neonatal human lung. J. Histochem. Cytochem. *44*, 673–678.

Stanfel, M.N., Moses, K.A., Schwartz, R.J., and Zimmer, W.E. (2005). Regulation of organ development by the NKX-homeodomain factors: an NKX code. Cell. Mol. Biol. (Noisy-le-grand) (*Suppl 51*), OL785–OL799.

Tagne, J.B., Gupta, S., Gower, A.C., Shen, S.S., Varma, S., Lakshminarayanan, M., Cao, Y., Spira, A., Volkert, T.L., and Ramirez, M.I. (2012). Genome-wide analyses of Nkx2-1 binding to transcriptional target genes uncover novel regulatory patterns conserved in lung development and tumors. PLoS One *7*, e29907.

Takeuchi, T., Tomida, S., Yatabe, Y., Kosaka, T., Osada, H., Yanagisawa, K., Mitsudomi, T., and Takahashi, T. (2006). Expression profile-defined classification of lung adenocarcinoma shows close relationship with underlying major

genetic changes and clinicopathologic behaviors. J. Clin. Oncol. *24*, 1679–1688.

Tanaka, H., Yanagisawa, K., Shinjo, K., Taguchi, A., Maeno, K., Tomida, S., Shimada, Y., Osada, H., Kosaka, T., Matsubara, H., et al. (2007). Lineage-specific dependency of lung adenocarcinomas on the lung development regulator TTF-1. Cancer Res. *67*, 6007–6011.

Watanabe, H., Francis, J.M., Woo, M.S., Etemad, B., Lin, W., Fries, D.F., Peng, S., Snyder, E.L., Tata, P.R., Izzo, F., et al. (2013). Integrated cistromic and expression analysis of amplified NKX2-1 in lung adenocarcinoma identifies LMO3 as a functional transcriptional target. Genes Dev. *27*, 197–210.

Weir, B.A., Woo, M.S., Getz, G., Perner, S., Ding, L., Beroukhim, R., Lin, W.M., Province, M.A., Kraja, A., Johnson, L.A., et al. (2007). Characterizing the cancer genome in lung adenocarcinoma. Nature *450*, 893–898.

Wert, S.E., Dey, C.R., Blair, P.A., Kimura, S., and Whitsett, J.A. (2002). Increased expression of thyroid transcription factor-1 (TTF-1) in respiratory epithelial cells inhibits alveolarization and causes pulmonary inflammation. Dev. Biol. *242*, 75–87.

Winslow, M.M., Dayton, T.L., Verhaak, R.G., Kim-Kiselak, C., Snyder, E.L., Feldser, D.M., Hubbard, D.D., DuPage, M.J., Whittaker, C.A., Hoersch, S., et al. (2011). Suppression of lung adenocarcinoma progression by Nkx2-1. Nature *473*, 101–104.

Yamaguchi, T., Yanagisawa, K., Sugiyama, R., Hosono, Y., Shimada, Y., Arima, C., Kato, S., Tomida, S., Suzuki, M., Osada, H., and Takahashi, T. (2012). NKX2-1/TITF1/TTF-1-induced ROR1 is required to sustain EGFR survival signaling in lung adenocarcinoma. Cancer Cell *21*, 348–361.

Yan, C., and Whitsett, J.A. (1997). Protein kinase A activation of the surfactant protein B gene is mediated by phosphorylation of thyroid transcription factor 1. J. Biol. Chem. *272*, 17327–17332.

Yan, C., Naltner, A., Conkright, J., and Ghaffari, M. (2001). Protein-protein interaction of retinoic acid receptor α and thyroid transcription factor-1 in respiratory epithelial cells. J. Biol. Chem. *276*, 21686–21691.

Yan, C., Naltner, A., Martin, M., Naltner, M., Fangman, J.M., and Gurel, O. (2002). Transcriptional stimulation of the surfactant protein B gene by STAT3 in respiratory epithelial cells. J. Biol. Chem. *277*, 10967–10972.

Yang, L., Yan, D., Bruggeman, M., Du, H., and Yan, C. (2004). Mutation of a lysine residue in a homeodomain generates dominant negative thyroid transcription factor 1. Biochemistry *43*, 12489–12497.

Yatabe, Y., Mitsudomi, T., and Takahashi, T. (2002). TTF-1 expression in pulmonary adenocarcinomas. Am. J. Surg. Pathol. *26*, 767–773.

Yatabe, Y., Kosaka, T., Takahashi, T., and Mitsudomi, T. (2005). EGFR mutation is specific for terminal respiratory unit type adenocarcinoma. Am. J. Surg. Pathol. *29*, 633–639.

Yin, Z., Gonzales, L., Kolla, V., Rath, N., Zhang, Y., Lu, M.M., Kimura, S., Ballard, P.L., Beers, M.F., Epstein, J.A., and Morrisey, E.E. (2006). Hop functions downstream of Nkx2.1 and GATA6 to mediate HDAC-dependent negative regulation of pulmonary gene expression. Am. J. Physiol. Lung Cell. Mol. Physiol. *291*, L191–L199.

Yuan, B., Li, C., Kimura, S., Engelhardt, R.T., Smith, B.R., and Minoo, P. (2000). Inhibition of distal lung morphogenesis in Nkx2.1(−/−) embryos. Dev. Dyn. *217*, 180–190.

Zhou, B., Zhong, Q., Minoo, P., Li, C., Ann, D.K., Frenkel, B., Morrisey, E.E., Crandall, E.D., and Borok, Z. (2008). Foxp2 inhibits Nkx2.1-mediated transcription of SP-C via interactions with the Nkx2.1 homeodomain. Am. J. Respir. Cell Mol. Biol. *38*, 750–758.

doi: 10.1111/j.1472-8206.2012.01056.x

ORIGINAL ARTICLE

Thymoquinone as an anticancer agent: evidence from inhibition of cancer cells viability and invasion in vitro and tumor growth *in vivo*

Samir Attoub[a]*, Olivier Sperandio[b], Haider Raza[c], Kholoud Arafat[a], Suhail Al-Salam[d], Mahmood Ahmed Al Sultan[a], Maha Al Safi[a], Takashi Takahashi[e] and Abdu Adem[a]

[a]*Department of Pharmacology & Therapeutics, Faculty of Medicine & Health Sciences, United Arab Emirates University, PO Box: 17666, Al Ain, United Arab Emirates*

[b]*INSERM UMR-S973/MTi, Université Paris Diderot, Bâtiment Lamarck, 35 Rue Hélène Brion, 75205 Paris Cedex 13, France*

[c]*Department of Biochemistry, Faculty of Medicine & Health Sciences, United Arab Emirates University, PO Box 17666, Al Ain, United Arab Emirates*

[d]*Department of Pathology,Faculty of Medicine & Health Sciences, UAE University, PO Box 17666, Al Ain, United Arab Emirates*

[e]*Division of Molecular Carcinogenesis, Center for Neurological Diseases and Cancer, Nagoya University Graduate School of Medicine, 65 Tsurumai-cho, Showa-ku, Nagoya, 466-8550, Japan*

Keywords
DNA damage,
invasion,
lung & breast cancer,
thymoquinone,
tumor growth,
viability

Received 11 March 2012;
revised 9 May 2012;
accepted 4 June 2012

*Correspondence and reprints:
samir.attoub@uaeu.ac.ae

ABSTRACT

Phytochemical compounds are emerging as a new generation of anticancer agents with limited toxicity in cancer patients. The purpose of this study was to investigate the potential impact of thymoquinone (TQ), the major constituent of black seed, on survival, invasion of cancer cells in vitro, and tumor growth *in vivo*. Exposure of cells derived from lung (LNM35), liver (HepG2), colon (HT29), melanoma (MDA-MB-435), and breast (MDA-MB-231 and MCF-7) tumors to increasing TQ concentrations resulted in a significant inhibition of viability through the inhibition of Akt phosphorylation leading to DNA damage and activation of the mitochondrial-signaling proapoptotic pathway. We provide evidence that TQ at non-toxic concentrations inhibited the invasive potential of LNM35, MDA-MB-231, and MDA-MB231-1833 cancer cells. Moreover, we demonstrate that TQ synergizes with DNA-damaging agent cisplatin to inhibit cellular viability. The anticancer activity of thymoquinone was also investigated in athymic mice inoculated with the LNM35 lung cells. Administration of TQ (10 mg/kg/i.p.) for 18 days inhibited the LNM35 tumor growth by 39% ($P < 0.05$). Tumor growth inhibition was associated with significant increase in the activated caspase-3. The *in silico* target identification suggests several potential targets of TQ mainly HDAC2 proteins and the 15-hydroxyprostaglandin dehydrogenase. In this context, we demonstrated that TQ treatment resulted in a significant inhibition of HDAC2 proteins. In view of the available experimental findings, we contend that thymoquinone and/or its analogues may have clinical potential as an anticancer agent alone or in combination with chemotherapeutic drugs such as cisplatin.

INTRODUCTION

Cancer is a leading cause of death worldwide and remains a therapeutic enigma. Among different forms of cancer, lung cancer is the most common with the highest mortality rate, and colorectal cancer is the second cause of cancer-related death after lung cancer in men and breast cancer in women. Hepatocellular carcinoma is also a common cancer in Asia and Africa and one of the most common causes of cancer-related mortality worldwide, accounting for about half a million deaths annually [1]. Despite advances in molecular biology of cancer, improved diagnosis, and new targeted therapies, the cure of lung, breast, and colon cancer remain elusive. To improve the survival of cancer patients, we need to develop new cytotoxic compounds and make use of selective molecular targeting anticancer drugs.

Over recent years, growing interest in phytochemical compounds with anticancer potential has been observed stimulating more in vitro and preclinical screening of these compounds. Thymoquinone (TQ), the most abundant constituent of black seed (*Nigella Sativa*), has been shown to exert anti-inflammatory, anti-oxidant, and antineoplastic effects both in vitro and *in vivo* [2,3]. TQ has been shown to inhibit cellular proliferation and induce apoptosis in human colon, breast, brain, pancreatic, and ovarian cancer cell lines [3–6]. The numerous reports on the protective effect of thymoquinone against drug-induced toxicity suggest a possible role of thymoquinone as an adjuvant in improving the quality of life of cancer patients [3]. In this study, we investigated the impact of thymoquinone on human cancer cell survival, and invasion in vitro and tumor xenograft growth *in vivo*. Our results showed a dramatic anticancer effect of TQ on a variety of tumor cells under in vitro as well as on lung tumor growth *in vivo*. We have also hypothesized functional targets that may potentially be affected by TQ using *in silico*-based protein data bank.

MATERIALS AND METHODS

Cell culture and reagents

Human lung cancer cells LNM35 (NSCLC) [7] were maintained in RPMI 1640 (Invitrogen, Paisley, UK); human hepatoma cells HepG2, human colorectal cancer cells HT29, human mammary adenocarcinoma cells (MCF-7, MDA-MB-231, and MDA-MB-213-1833), and human melanoma MDA-MB-435 were maintained in DMEM (Invitrogen). All media were supplemented with 10% fetal bovine serum (Roche Molecular Biochemicals, Meylan, France). Thymoquinone was purchased from Sigma-Aldrich (Saint-Quentin Fallavier, France).

Primary antibodies were purchased from the following manufacturers: polyclonal antibodies for cytochrome *c*, poly (ADP-ribose) polymerase (PARP), and HDAC2 (Santa Cruz, CA, USA), Bcl-2, phosphor-Akt (Cellular Signaling Technology, Beverly, MA, USA), phospho-histone H2a.X (Millipore, Hayward, CA, USA), and monoclonal rat anti-mouse CD31 antibody (BD Pharmingen, San Jose, CA, USA). The secondary antibodies were goat anti-rat antibody (Sigma, Saint Louis, MO, USA) and rabbit anti-mouse antibody (Dako, Copenhagen, Denmark). Signal Stain Cleaved Caspase-3 (Asp175) IHC detection kit was purchased from Cellular Signaling Technology).

Cellular viability

Cells were seeded at 5000 cells/well in 96-well plate. After 24 h, cells were treated for another 24 h with increasing concentrations of thymoquinone (1–100 μM) in triplicates. Control cultures were treated with 0.1% DMSO. The effect of thymoquinone on cell viability was determined using a CellTiter-Glo luminescent cell viability assay (Promega Corporation, Madison, WI, USA), based on quantification of ATP, which signals the presence of metabolically active cells. Luminescent signal was measured using GLOMAX Luminometer system. The data were presented as proportional viability (%) by comparing the treated group with the untreated cells, the viability of which is considered as 100%.

Caspase-3/7 activity

Cells were seeded at a density of 5000 cells/well into 96-well plate and treated with 10 μM of thymoquinone (HepG2) and with 100 μM of thymoquinone for 24 h (LNM35), in triplicate assays. Caspase-3/7 activity was measured using a luminescent Caspase-Glo 3/7 assay kit following manufacturer's instructions (Promega Corporation). Caspase reagent was added, and the plate was mixed using an orbital shaker and incubated for 2.5 h at room temperature. Luminescence was measured using a GLOMAX Luminometer system (Promega, Madison, WI, USA).

Expression of apoptotic and DNA damage protein members

LNM35 and MDA-MB-231 cells were seeded in 100 mm dishes at 3×10^6 cells/dish for 24 h and with

increasing concentrations of thymoquinone (1–50 μM) for 30 min, 2, 6, and 24 h. Total cellular proteins were isolated using RIPA buffer (25 mM Tris–HCl pH 7.6, 1% nonidet P-40, 1% sodium deoxycholate, 0.1% SDS, 0.5% protease inhibitors cocktail, 1% PMSF, 1% phosphatase inhibitors cocktail) from control and treated cells. The whole cell lysate was recovered by centrifugation at 23 000 g for 20 min at 4 °C to remove insoluble material, and 50 μg of protein was separated by a 10% SDS gel for phospho-Akt and HDAC2 and 12% SDS gel for Anti-phospho-Histone H_2aX. After electrophoresis, the proteins were transferred on a nitrocellulose membrane, blocked with 5% non-fat milk and probed with $pSer^{473}$-Akt (1 : 1000), H_2aX (1 : 500), HDAC2 (1 : 200), and β-actin (1 : 1000) antibodies overnight at 4 °C. The blot was washed, exposed to horseradish peroxidase (HRP)-conjugated secondary antibodies, and visualized using the ECL system (Santa Cruz).

For the expression of cytochrome *c*, PARP, and Bcl-2, the cells were seeded in 100 mm dishes at 3×10^6 cells/dish and treated with 10 μM of thymoquinone for 6 and 24 h. After, cells were harvested, washed with PBS (pH 7.4), and homogenized in mitochondrial isolation H-medium buffer (70 mM sucrose, 220 mM mannitol, 2.5 mM HEPES, 2 mM EDTA) and 0.1 mM phenylmethylsulfonylfluoride at 4 °C. Mitochondria and postmitochondrial supernatants (PMS) were prepared by centrifugation, and the purity of the mitochondrial fraction was ascertained by assaying for organelle-specific marker enzymes as described previously [8]. Mitochondrial preparations containing <3% cross-contamination were used in experiments. Proteins (50 μg) from mitochondria and PMS were separated on 12% SDS-PAGE and electrophoretically transferred onto nitrocellulose paper by Western blotting. The immunoreacting protein bands were visualized after interacting with primary antibodies against cytochrome *c* and PARP and Bcl-2 as described before [9].

Wound healing motility assay

LNM35 and MDA-MB-231 cells were grown in six-well tissue culture dishes until they reach confluence. A scrape was made through the confluent monolayer with a plastic pipette tip of 1-mm diameter. Afterwards, dishes were washed twice and incubated at 37 °C in fresh RPMI containing 10% fetal calf serum in the presence or absence of the indicated concentrations of thymoquinone (1 and 10 μM). At the bottom side of each dish, two arbitrary places were marked where the width of the wound was measured with an inverted microscope (4×). Motility was expressed as the average ± SEM of the difference between the measurements at time zero and the 2–24 h time period.

Matrigel and Oris invasion assays

The invasiveness of the lung cancer cells LNM35 and breast cancer cells MDA-MB-231 treated with thymoquinone (1 and 10 μM) was tested using BD Matrigel Invasion Chamber (8-μm pore size; BD Biosciences, Le Pont de Claix, France). The PI3′-K inhibitor LY294002 (20 and 50 μM, respectively) was used as a positive inhibitor of cellular invasion. Cells (1×10^5 cells in 0.5 mL of media and the indicated concentration of thymoquinone) were seeded into the upper chambers of the system, and the bottom wells in the system were filled with RPMI supplemented with 10% fetal bovine serum as a chemo-attractant and then incubated at 37 °C for 24 h. Non-penetrating cells were removed from the upper surface of the filter with a cotton swab. Cells that have migrated through the matrigel were fixed with 4% formaldehyde, stained with DAPI, and counted in 20 random fields under a microscope. For quantification, the assay was performed in duplicates and repeated three times.

The Oris™ Cell Invasion Assay (AMS Biotechnology, Abingdon, UK) was used to investigate the impact of thymoquinone on MDA-MB-231-1833 cell invasion in vitro within a 3-dimensional extracellular matrix comprised of a basement membrane extract (BME) of the murine Engelbreth-Holm-Swarm tumor. Cells were seeded at 100 000 cells/well and allowed to attach overnight onto plates coated with BME solution. Once the cells formed a confluent monolayer, the silicone stoppers were removed and the cells treated with thymoquinone (1 and 10 μM) or the PI3′-K inhibitor LY294002 (20 μM). Following 48 h invasion, cells were labeled with Calcein AM (Invitrogen, CA, USA), and images were acquired, in the absence of the mask, by use of an Olympus fluorescence microscope.

Tumor growth and metastasis assay

Six-week-old athymic NMRI female nude mice (nu/nu, Elevage Janvier, France) were housed in filtered-air laminar flow cabinets and handled under aseptic conditions. Procedures involving animals and their care were conducted in conformity with Institutional guidelines that are in compliance with Faculty of

Medicine and Health Sciences, UAEU, National and International laws and policies (EEC Council Directive 86/609, OJ L 358, 1, December 12, 1987; and NIH Guide for Care and Use of Laboratory Animals, NIH Publication No. 85–23, 1985). Human Pulmonary LNM35 cells (1×10^6 cells) were injected subcutaneously into the lateral flank of the nude mice. One week after inoculation, when tumors had reached the volume of approximately 100 mm^3, animals (six in each group) were treated with thymoquinone (10 mg/kg, i.p.) or control (vehicle alone) 3 days per week (Sunday, Tuesday, and Thursday) for a total of 18 days. Tumor dimensions were measured with calipers every 3 days. Tumor volume (V) was calculated using the formula: $V = 0.4 \times a \times b^2$, with '$a$' being the length and '$b$' the width of the tumor. The animals were killed 18 days after treatment initiation, and the tumors and the axillary lymph nodes were excised, weighed, and fixed for immunohistochemical analysis.

Immunohistochemical determination of CD31/platelet-endothelial cell adhesion molecule 1 (PECAM-1) for microvessel density and cleaved caspase-3 for apoptotic cells

The effect of thymoquinone on angiogenesis was evaluated using CD31 immunostaining. The tumor tissues were quickly frozen in isopentane at −130 °C and stored at −70 °C until further processing. The frozen sections (8 μm) were fixed in acetone and incubated overnight with a CD31 antibody (1 : 400). Slides were then washed three times in PBS and incubated with secondary antibody (goat anti-rat 1 : 200) for one hour at room temperature. The sections were then stained with DAB and counterstained with hematoxylin. Vessel density was determined by counting the number of microvessels. The area occupied by CD31-positive microvessels and total tissue area per section were quantified and compared between treated and control mice. For individual tumors, the microvessel count was scored by averaging the counts from all fields. All analyses were performed in a blind fashion. The paraffin-embedded tissue sections (5 μm) were deparaffinized and then microwaved for 5 min for antigen retrieval. For the identification of apoptotic cells, cleaved caspase-3 staining was performed following the instructions of a commercially available Signal Stain Cleaved Caspase-3 (Asp175) IHC detection kit (Cellular SignalingTechnology, Beverly, MA, USA). Ten high-power fields (0.159 mm^2) per section of four to five tumors per treatment group were examined microscopically, and the average number of cells that stained positive for cleaved caspase-3 per treatment group was evaluated.

TarFisDock is a web-based tool for automating the procedure of searching for small molecule–protein interactions over a large repertoire of protein structures. It offers PDTD (potential drug target database), a target database containing 698 protein structures covering 15 therapeutic areas and a reverse ligand–protein docking program [10].

Potential Drug Target Database (PDTD) is a web-accessible protein database for *in silico* target identification. It currently contains >1100 protein entries with 3D structures presented in the Protein Data Bank. Data are extracted from the literatures and several online databases such as TTD, DrugBank, and Thomson Pharma. The database covers diverse information of >830 known or potential drug targets, including protein and active sites' structures in both PDB and mol2 formats, related diseases, biological functions as well as associated regulating (signaling) pathways. Each target is categorized by both nosology and biochemical function. In conjunction with TarFisDock, PDTD can be used to identify binding proteins for small molecules. The results can be downloaded in the form of mol2 file with the binding pose of the probe compound and a list of potential binding targets according to their ranking scores [11].

Statistical analysis

Results were expressed as means ± SEM. The difference between experimental and control values were assessed by ANOVA followed by Dunnett post hoc multiple comparison test. Tumor growth assays were analyzed using the unpaired Student's t-test. $P < 0.05$ indicates a significant difference.

RESULTS

Effect of thymoquinone on cell viability

As shown in *Figure 1*, exposure of LNM35, HepG2, HT29, MDA-MB-435, MDA-MB-231, and MCF-7 cells to increasing TQ concentrations (1–100 μM) for 24 h decreased cellular viability in a concentration-dependent manner. The IC_{50} concentrations (producing half-maximal inhibition) at 24 h were between 50 and 78 μM of TQ for all cells except for HepG2, and the IC_{50} was 34 μM of TQ. HepG2 cells seem to be the more sensitive cells to the cytotoxic effects of thymoquinone.

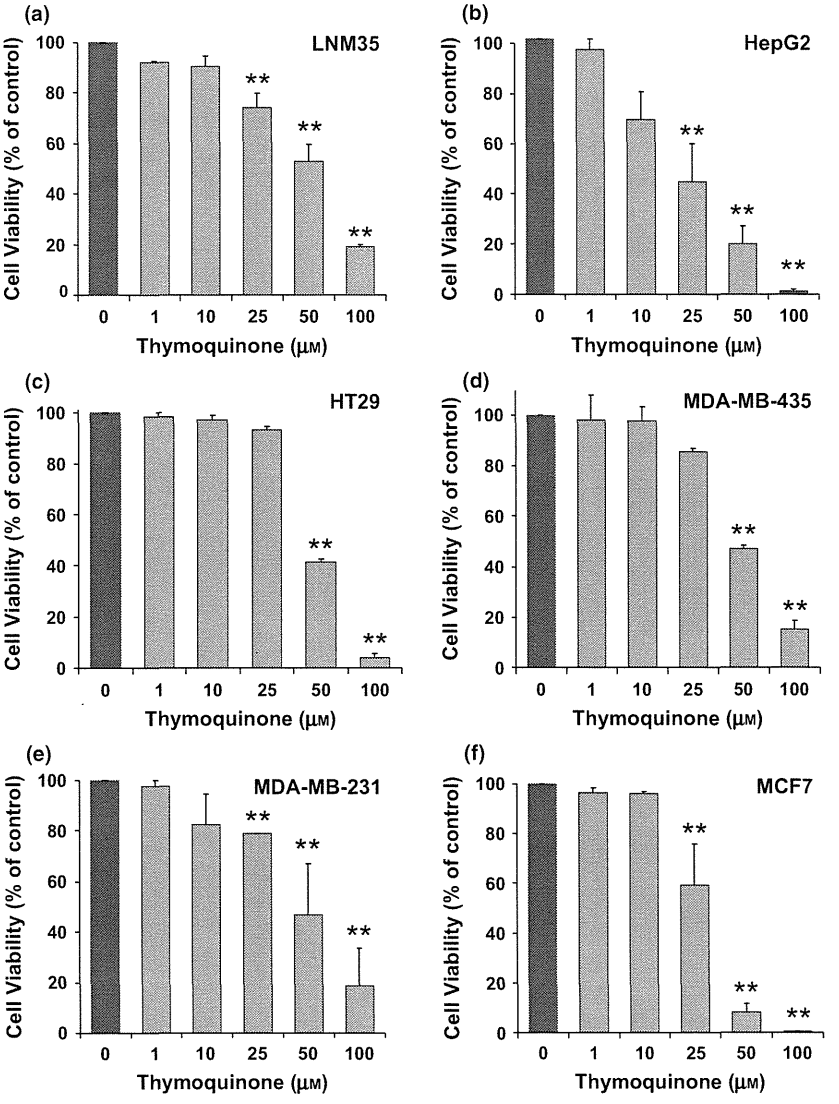

Figure 1 Inhibition of cellular viability by thymoquinone. Exponentially growing LNM35, HepG2, HT29, MDA-MB-435, MDA-MB-231, and MCF7 cells were treated for 24 h with vehicle (0.1% DMSO) and the indicated concentrations of thymoquinone. Viable cells were assayed as described in Materials and Methods. All experiments were repeated at least three times. *Columns*, mean; *bars*, SEM. **Significantly different at $P < 0.01$.

TQ treatment inhibits Akt phosphorylation and induces DNA damage in both MDA-MB-231 and LNM35 cancer cells

Phosphorylated Akt promotes cancer cell survival by inhibiting downstream apoptotic targets, such as proapoptotic Bcl-2 family member BAD and GSK-3 and increasing the survival targets such as Bcl-2. In this context, inhibition of the Akt pathway has been targeted as a promising strategy for cancer therapy. LNM35 and MDA-MB-231 cells were exposed to increasing concentrations of TQ for 30 min, 2, 6, and 24 h and total proteins were evaluated for phosphorylated Akt on serine 473. In both LNM35 and MDA-MB-231 cells, TQ induces a clear concentration and time-dependent inhibition of p-Akt (*Figure 2a*). These results indicate that the induction of apoptosis by TQ is at least in part associated with reduction in activated survival kinase Akt.

To check whether the induction of cell death by TQ is because of DNA damage, LNM35 as well as MDA-MB-231 cells were exposed to increasing concentrations of TQ for 30 min, 2, 6, and 24 h and total proteins were evaluated for γ-H_2aX expression. In both LNM35 and MDA-MB-231 cells, TQ induces a concentration and time-dependent increase in γ-H_2aX expression indicating that cell death induced by TQ was associated with induction of DNA damage (*Figure 2b*).

Cytochrome *c* release from mitochondria, caspase-3/7, and PARP activation

HepG2, the more sensitive cells to the cytotoxic effect of TQ, were used to determine whether the thymoquinone

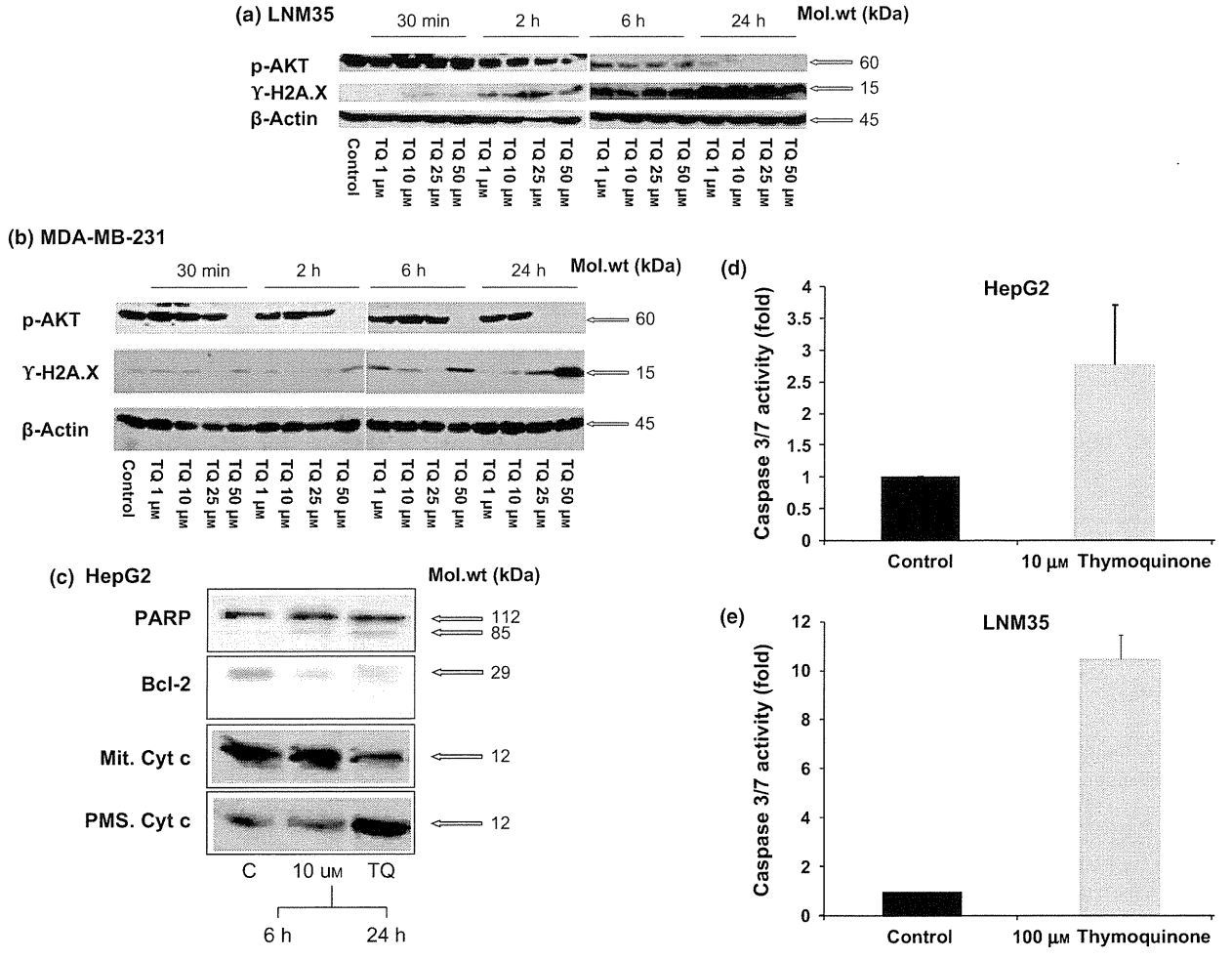

Figure 2 Phosphorylation of Akt and H_2aX, cytochrome *c* release, induction of caspase-mediated apoptosis PARP activation by thymoquinone. Indicated cells were exposed to increasing concentrations of TQ, and total proteins were collected after 30 min, 2, 6, and 24 h, and the phosphorylation of Akt and H_2aX protein was assessed by immunoblot in (a) LNM35 and (b) MDA-MB-231 cells. (c) Human hepatoma cancer cells HepG2 were treated with vehicle (0.1% DMSO) or 10 µM of thymoquinone for 6 h. c, upper panel) PARP cleavage in HepG2 cells treated with thymoquinone 10 µM and incubated for incubated for 6 and 24 h. Cleavage of PARP was detected by Western blotting; 112- and 85-kDa protein bands indicated native and cleaved PARP, respectively. c, lower panel) Cytochrome *c* expression in the mitochondria and postmitochondrial supernatants (PMS). (d) Induction of caspase-3/7 activity by thymoquinone in HepG2 cells and (e) in LNM35 cells. Caspase-3/7 activity was determined using the Caspase-Glo 3/7 assay and was normalized to the number of viable cells per well and expressed as fold induction compared with the control group.

effect was because of apoptosis. Western blot analysis of the HepG2 cells revealed that 6 and 24 h treatment with 10 µM thymoquinone caused an increase in the release of cytochrome *c* from the mitochondria as compared to the control cells (*Figure 2c*). In a sequential manner, once the cytochrome *c* released into cytosol, it recruits and activates caspases that are the executioners of apoptosis. To determine whether cells were undergoing apoptosis, the activity of the main effector caspases, caspases-3 and -7, was analyzed using the Caspase-Glo 3/7 assay 6 h after treatment with TQ (10 µM). The relative caspase activity was normalized to the number of cells per well and compared to the control cells. A significant 2.7 fold increase in caspase-3 and -7 activities was observed in HepG2 cells (*Figure 2d*). To confirm that LNM35 cells also were undergoing apoptosis after exposure to thymoquinone, caspase-3/7 was measured 24 h after treatment with TQ (100 µM). A 10 folds increase in caspase-3/7 activity was observed in LNM35 cells after treatment with TQ

100 μM (*Figure 2e*). Poly-(ADP-ribose) polymerase-1 (PARP-1) is a nuclear enzyme involved in DNA repair and stability downstream of caspase-3/7 activation. Cleavage of PARP-1 is used as a hallmark of caspase-3/7 activation and apoptosis. PARP-1 cleavage during apoptosis impairs the DNA repair capacity of the cell. Intact PARP (112 kDa) was seen in DMSO-treated HepG2 cells. However, after 6 and 24 h treatment of HepG2 cells with 10 μM of thymoquinone, PARP was cleaved into an 85 kDa fragment as a result of caspase-3/7 activation and which is consistent with cell death that results from apoptosis (*Figure 2c*). We also demonstrated a reduced expression of BcL-2 in HepG2 cells after TQ treatment (*Figure 2c*).

Impact of thymoquinone on cancer cell motility and invasion

Using a classic in vitro wound healing model, we assessed whether thymoquinone was able to inhibit epithelial cell motility. Thymoquinone was found to be ineffective in reducing cellular motility in the LNM35 cells (*Figure 3a*); similarly, the dose- and time-dependant inhibition observed in the MDA-MB-231 was also not statistically significant even after 6 h incubation with TQ 10 μM (*Figure 3b*).

However, TQ was able to significantly reduce the invasiveness of both LNM35 and MDA-MB-231 cells in matrigel invasion assay (*Figure 4a,b*). The inhibition of matrigel invasion seen following exposure of cells to low concentrations of TQ (0.1, 1, and 10 μM) occurred

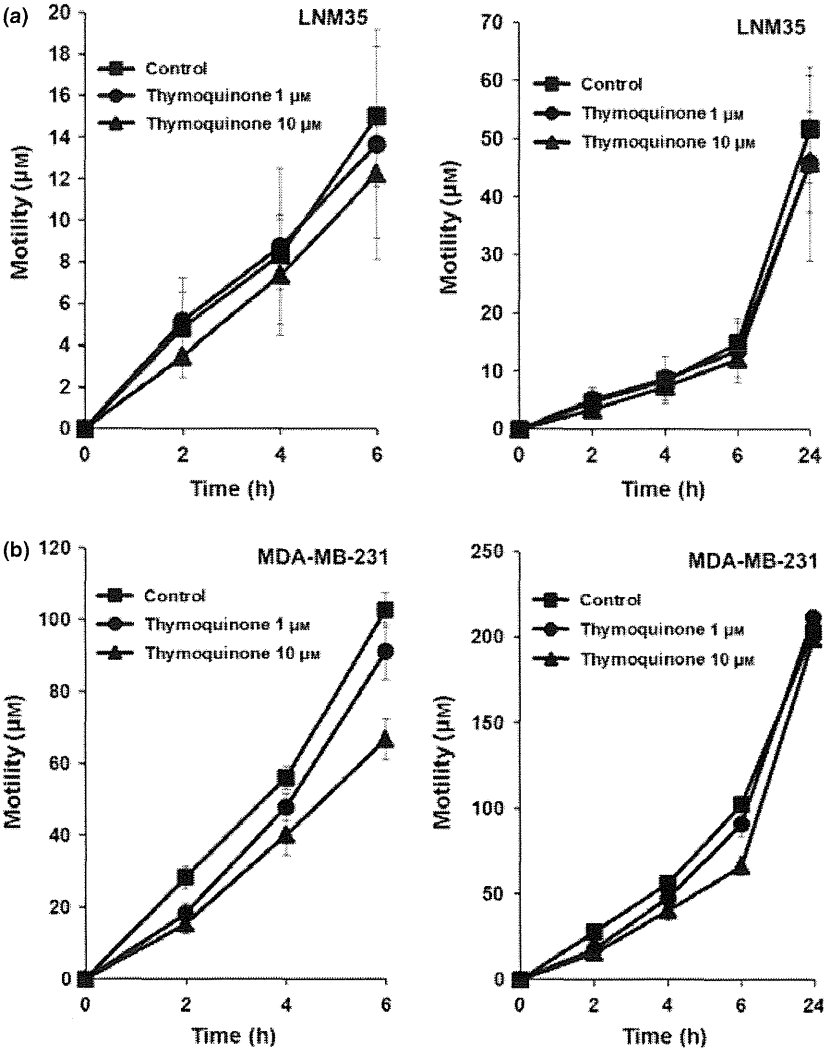

Figure 3 Dose–response effect of thymoquinone on cellular motility. Wounds were introduced in confluent monolayers LNM35 (a) and MDA-MB-231 (b) cells in the presence or absence (control) of thymoquinone (1 and 10 μM). The mean distance that cells travelled from the edge of the scraped area for 2, 4, 6, and 24 h at 37 °C was measured in a blinded fashion, using an inverted microscope (4× magnifications). Data are means ± SEM of two independent experiments.

without reduction in cell viability (*Figure 1a,e*). Next, we investigated the impact of non-toxic concentration of 1 μM of TQ (*Figure 4c*) on the invasiveness of the highly invasive breast cancer cells MDA-MB231-1833 using Oris invasion assay. Again, TQ reduced the invasiveness of these cells at the non-toxic concentration of 1 μM (*Figure 4d*). We conclude that TQ significantly reduced the invasive potential of lung cancer (LNM35) and breast cancer (MDA-MB231 and MDA-MB231-1833) cells.

In vivo impact of thymoquinone on tumor growth

The anticancer activity of TQ was investigated in athymic mice inoculated with the highly tumorigenic LNM35 human lung cells as xenografts. TQ reduced the growth of LNM35 human tumor xenografts by 39% at day 18 (*Figure 5a*). There was no sign of toxicity because of thymoquinone administration and no significant difference in body weight between the thymoquinone-treated animals and the control group (data not shown). The effect of TQ on tumor angiogenesis was assessed by CD31-immunostaining of LNM35 tumor tissue xenografts. CD31 is specifically expressed on the surface of endothelial cells and is weakly expressed on lymphoid cells and platelets. Immunohistochemical analysis indicated that when the CD31-positive areas or number of microvessels was normalized to tumor area, TQ vs. control did not cause vascular regression in the tumors. LNM35 tumor growth inhibition was associated with a significant increase in caspase-3 activity similar to the in vitro results indicating that the tumor growth inhibition induced by TQ is mainly due to the induction of apoptosis (*Figure 5b*). Next, we assessed the metastatic behavior of the human pulmonary cell

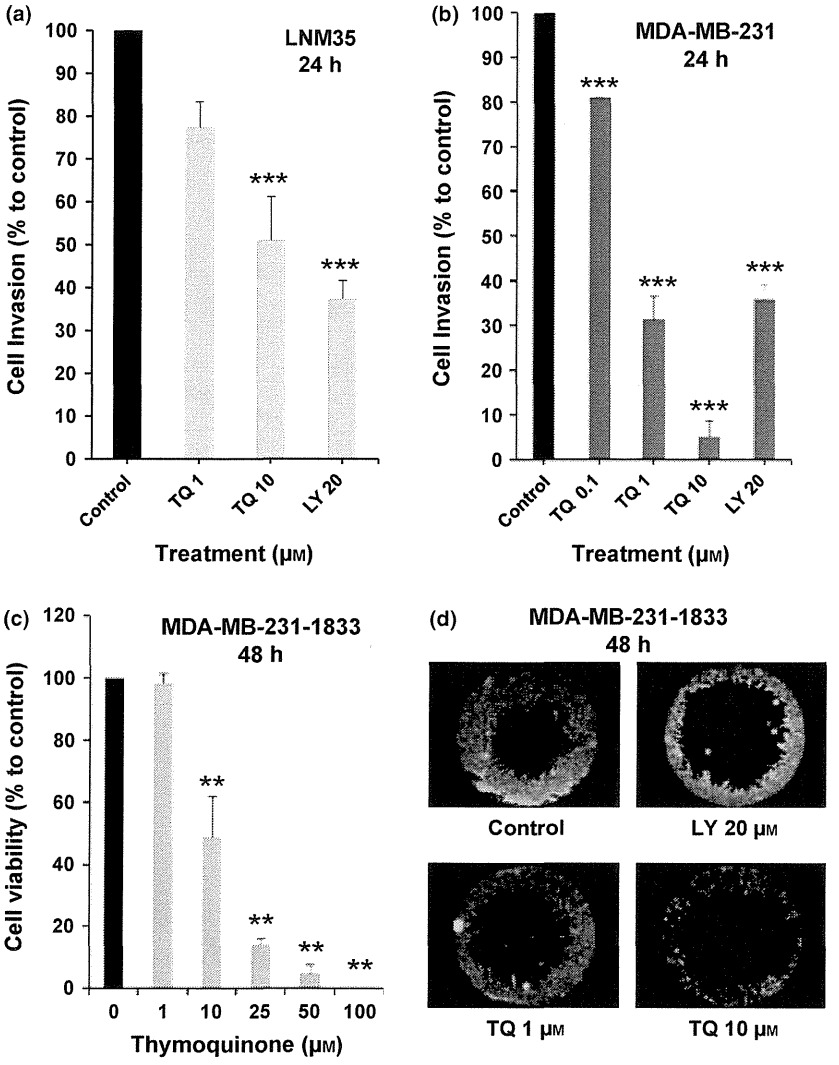

Figure 4 Dose effect of thymoquinone on matrigel and Oris cell invasion assay. (a) LNM35; (b) MDA-MB-231 cells were incubated for 24 h in the presence or absence of thymoquinone (0.1–10 μM). Cells that invaded into matrigel were scored as described in Materials and Methods. *Columns*, mean; bars, SEM. (c) MDA-MB-213-1833 cells were treated with vehicle for 48 h (0.1% DMSO) and the indicated concentrations of TQ. Viable cells were assayed as described in Materials and Methods. (d) MDA-MB-213-1833 cells were incubated for 48 h in the presence or absence of thymoquinone (1 and 10 μM), LY (20 μM) onto an Oris cell invasion assay plate. Cell invasion images were acquired by inverted microscope as described in Materials and Methods. Experiments were repeated at least three times. Columns, mean; bars, SEM. **Significantly different at $P < 0.01$, ***Significantly different at $P < 0.001$.

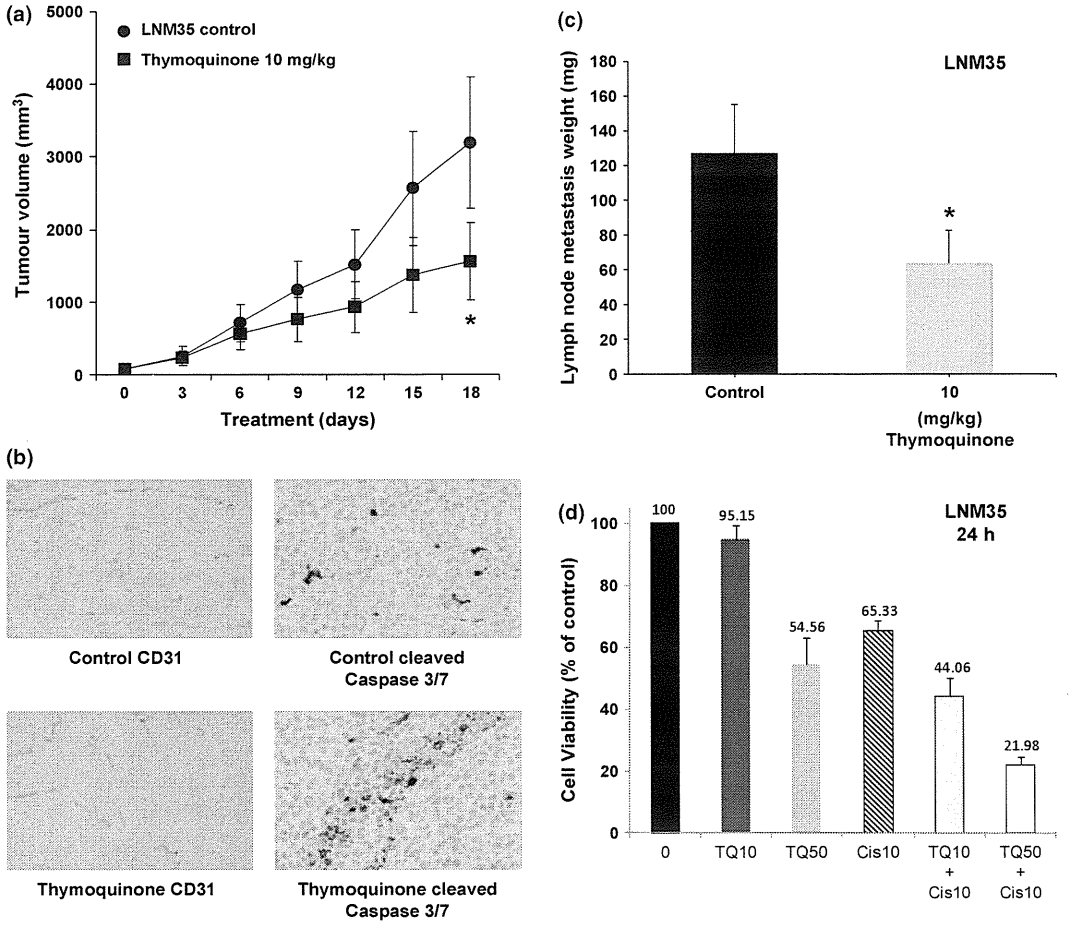

Figure 5 Impact of thymoquinone on the tumor volume, angiogenesis, cancer cell death, and metastasis of established human lung cancer xenografts. (a) Nude mice were xenografted S.C. with human lung LNM35 cancer cells (10^6 cells per animal) and treated with thymoquinone (10 mg/kg, i.p) or control (carrier solution alone) 3 days per week (Sunday, Tuesday, and Thursday) for a total of 18 days. Data points represent the mean ± SEM of 6 to 7 mice per group. Statistically significant differences are indicated in (a) for tumor volume (*$P < 0.05$ vs. control). (b) Immunohistochemical staining for CD31 (right panel) and cleaved caspase-3/7 (left panel) in LNM35 human lung cancer growing in nude mice treated with saline (control) and thymoquinone. (c) Lymph nodes metastasis weight of established human lung cancer xenografts treated with TQ 10 mg/kg for 18 days. *Columns*, mean; *bars*, SEM. (d) LNM35 cells were incubated in the presence or absence of thymoquinone (10 and 50 μM), cisplatin (10 μM) or with combined thymoquinone and cisplatin treatment for 24 h. Cell viability was measured as described in Materials and Methods. All experiments were repeated at least three times. *Columns*, mean; *bars*, SEM.

line LNM35 by examining axillary lymph nodes. In the control-treated group, the mean lymph nodes weight was 127 ± 28.1 mg compared with 63.5 ± 19.2 mg in the groups treated with TQ 10 mg/kg/day for 18 days (*Figure 5c*).

Thymoquinone synergizes with cisplatin to inhibit cellular viability

Our *in vivo* data encouraged us to investigate the possible contribution of TQ to enhance the cytotoxicity of cisplatin in the human NSCLC lung cell line LNM35 in vitro. Interestingly, low to moderate concentrations of TQ (10 and 50 μM) revealed a synergistic inhibition of LNM35 cell viability in vitro in combination with cisplatin (10 μM) (*Figure 5d*).

An attempt to identify a target for thymoquinone

In an attempt to suggest possible targets for thymoquinone, we carried out a short chemo-informatics study combining a reverse docking procedure and a ligand-based similarity approach. In the former approach, we used the TarFisDock web server to reverse dock TQ on

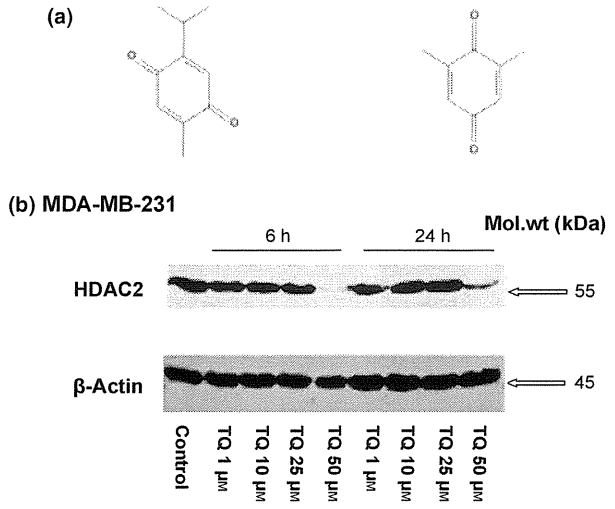

Figure 6 (a) 2D sketches of THQ (Left) and 2, 6-dimethyl-1, 4-benzoquinone (Right) that have a 0.84 pairwise Tanimoto coefficient. (b) MDA-MB-231 cells were exposed to increasing concentrations of TQ, and total proteins were collected after 6 and 24 h, and the expression of HDAC2 protein was assessed by immunoblot.

1207 different protein structures. This corresponds to 841 different protein targets spanning through a vast array of protein types and associated diseases. Among the results, we found several potential targets for TQ that are known to be involved cancer, such as Carboxypeptidase A (Pancreatic Cancer), Thymidine Kinase (Bladder Cancer), HDAC-2 (Colon Cancer), and Nuclear Vitamin D Receptor (Colorectal and Prostate Cancer). In the ligand-based similarity approach, we used the PubChem server to detect similar compounds to TQ (Tanimoto index above 0.8), and we analyzed the PubChem BioAssay results available for those compounds. Interestingly, only one compound, 2, 6-dimethyl-1, 4-benzoquinone (*Figure 6a*) has been identified as active within a PubChem Bioassay whose protein target was clearly identified (Pubchem Bioassay AID388). The associated target is the human 15-hydroxyprostaglandin dehydrogenase (HPGD). In this context, we demonstrated that TQ treatment for 6 and 24 h resulted in a significant inhibition of HDAC2 proteins (*Figure 6b*).

DISCUSSION

Nigella sativa popularly known as black seed has been used in traditional medicine for the treatment of a variety of illnesses, including bronchial asthma, headache, dysentery, infections, obesity, back pain, hypertension, gastrointestinal problems, and eczema [4]. Several bioactive components of black seed have been identified, including thymoquinone, thymol, thymohydroquinone, and dithymoquinone. Among them thymoquinone (TQ) has been reported to exhibit antioxidant, anti-inflammatory, and chemopreventive effects [3,4,12].

Results presented in this study demonstrate that thymoquinone induces cell death of several human cancer cell lines derived from lung, liver, colon, melanoma, and breast cancer. These results are in line with several other studies that have demonstrated that thymoquinone induced apoptosis in cancer cell lines including myeloblastic leukemia, pancreatic, ovarian, breast and colorectal adenocarcinoma [4,5,13–15].

Previous studies reported that thymoquinone induced apoptosis in tumor cells by suppressing COX-2, survivin, Bcl family proteins, STAT3 phosphorylation, NF-κB, Akt activation, extracellular signal-regulated kinase (ERK), and inhibition of telomerase activity leading to telomere shortening [6,12,16–19]. A recent study proposed a new mechanism for the antineoplastic effect of TQ. The authors demonstrate that treatment with TQ induced ROS generation, which increased JNK and ERK in an attempt to bypass the stress injury. However, ERK and JNK fail to confer a survival role, and the cells undergo apoptosis [20].

It has been reported that Akt activation may allow cells to evade the deleterious consequences of DNA damage, and consequently, the inhibition of Akt phosphorylation will markedly enhance DNA damage [21]. The γ-H_2aX, phosphorylated histone H_2AX, formation is an early chromatin modification event that follows initiation of DNA fragmentation during apoptosis before DNA repair. We present strong evidence that the antineoplastic effect of TQ is at least in part, associated with induction of the DNA damage protein H_2aX in both breast and lung cancer cells. These results are in line with similar finding in colon cancer cells [22]. In this context, we provided mechanistic evidences that TQ-induced cell death is mediated, at least in part, by inhibition of the phosphorylation of the survival serine threonine kinase Akt leading to phosphorylation of γ-H_2aX.

Induction of apoptosis is a key factor in the response of tumors to chemotherapy. Cells can respond to DNA damage either by undergoing cell cycle arrest, to facilitate DNA repair, or by undergoing cell suicide. Apoptosis is a major form of cell death involving the

mitochondria (intrinsic pathway) or death receptors (extrinsic pathway). The intrinsic pathway involves the release of cytochrome *c* from the intermembrane space of the mitochondria leading to the activation of downstream caspase-3/7 that leads to the cleavage of PARP and the death response [23]. In this context, we determined the nature of cell death induced by TQ in our cancer cells, which engages the mitochondrial pathway, allowing the release of cytochrome *c*. Our results also show that TQ activates the apoptotic pathway, as evidenced by the activation of caspase-3/7, the main effector of apoptosis. These results are in line with previous studies indicating that caspase-3 activation-mediated the TQ-induced apoptosis in myeloblastic leukemia HL-60 cells and human laryngeal carcinoma cells HEp-2 [15,24]. Caspase-3 recognizes the DEVD motif within the amino-terminal domain of PARP-1 and cleaves this nuclear enzyme between amino acids 214 and 215 [25]. In this study, a p85 protein band representing the caspase-3 cleaved PARP-1 was generated in HepG2 cells after exposure to TQ.

In this study, we reported that treatment with non-toxic concentrations of thymoquinone (0.01, 0.1 and 1 μM) inhibits the invasiveness of human lung cancer cells LNM35 and human mammary adenocarcinoma cells (MDA-MB-231 and MDA-MB-213-1833). This ability of low concentration of TQ (0.1–10 μM) to reduce the invasiveness of breast cancer cells was also reported recently [26]. In line with our results, recent studies indicated that thymoquinone exhibits significant inhibitory effect on HGF-induced HepG2 hepatoma cell motility and invasion; VEGF-induced PC3 prostate cancer cell motility, on human umbilical vein endothelial cell (HUVEC) motility and invasion and also glioblastoma cells associated with FAK, MMP-2, and MMP-9 downregulation [17,27]. Similarly, high concentration of TQ (20–80 μM) significantly inhibits mouse C26 colon cancer cell invasion, pancreatic cancer cell invasion and metastasis as well as human NCI-H460 lung cancer cell invasion [28]. Taken together, these results confirm that the impact of thymoquinone on cancer cell motility and invasion is not tissue specific and suggests a potent antimetastatic effect of TQ. In this context, we demonstrated that TQ significantly reduces metastasis *in vivo*.

The chemotherapeutic agents currently in use for lung cancer are still unsatisfactory because of associated co-lateral toxicity and drug-induced resistance that encouraged us to investigate *in vivo* the anticancer activity of thymoquinone in athymic mice xenografted with the LNM35 human lung cells. Previous reports have demonstrated that the LD50 of TQ after intraperitonial injection to mice were 104.7 mg/kg [29]. A phase I study conducted by Al-Amri and Bamosa had reported no significant systemic toxicities in adult patients with solid tumors or hematological malignancies who were treated with thymoquinone [30]. It was also found that the human body could tolerate a dose of thymoquinone up to 2600 mg/day [3]. We demonstrated that intraperitonial administration of thymoquinone (10 mg/kg, 10 times less that the LD50 dose) for 18 days slows down LNM35 lung tumor growth by 39% without manifest side effects. It has also been demonstrated previously that thymoquinone (10 mg/kg) does not induce mortality or any pathological abnormalities in the lung, heart, or kidneys [31]. Our findings are in agreement with other studies showing that TQ (5–20 mg/kg/day) inhibits growth of HCT116 colon cancer and PC3 prostate cancer xenografts [17,28,32]. To determine the mechanism by which thymoquinone inhibits tumor growth, we investigated the impact of this compound on tumor cell survival and angiogenesis using cleaved caspases-3 and CD31 antibodies, respectively. We found that the tumor growth inhibition was associated with significant increase in apoptosis as reported in colon cancer xenografts treated with TQ [28], in contrast with previous report related to potential antiangiogenic effect of TQ [17]. In this study, the antineoplastic effect of TQ does not appear to be due to the inhibition of angiogenesis. At least at the dose of TQ used, no significant difference in neo-angiogenesis was observed between TQ and control LNM35 tumor xenografts.

Clinical trials revealed that single agent treatments rarely result in clinical benefits to cancer patients, suggesting that combination therapy is necessary for effective treatment for majority of cancers. Emerging evidence demonstrates that thymoquinone in combination with gemcitabine and/or oxaliplatin is superior as an antitumor agent compared with either agent alone [16]. It has been reported that TQ potentiates the antitumor activity of cisplatin and improves its therapeutic index in Ehrlich ascites carcinoma and also reduces the toxic effects of various anticancer drugs including cisplatin and doxorubicin [33,34]. Cisplatin is widely used in the treatment of lung, bladder, ovarian, and cervical cancer [35]. The first-line chemotherapeutic protocol in lung cancer is cisplatin in combination with paclitaxel, docetaxel, vinorelbine, gemcitabine, or irinotecan [36]. We examined the

possibility to enhance lung cancer cell death of cisplatin by combination with TQ. Our in vitro data indicate that combination of TQ and cisplatin caused greater inhibition of LNM35 lung cancer cell viability than each drug given alone. Recent study also showed a synergism between TQ and cisplatin in inhibition of the NCI-H460 lung cell proliferation as well as tumor growth [31]. Building on aforementioned results, which strongly support better killing of lung cancer cells when exposed to both cisplatin and thymoquinone, we will evaluate in future plan the therapeutic advantage of combination of cisplatin and thymoquinone in nude mice bearing LNM35 xenografts.

Interestingly, the identification of HDAC-2 among the potential protein targets and the demonstration in this study that TQ treatment leads to a decrease in HDAC2 protein level corroborates the recent findings suggesting that TQ inhibits histone deacetylase (HDAC) activity and induces histone hyperacetylation [37]. On the other hand, the human 15-hydroxyprostaglandin dehydrogenase (HPGD) is a target that has been recently associated with higher risk for colorectal cancer [38], and it is now known that TQ can inhibit tumor growth in murine colon cancer models [28]. Taken together, these preliminary results suggest several potential targets (mainly HDAC proteins and HPGD) and seem to corroborate the previously published studies on the effect of TQ cancer progression.

In conclusion, we provide evidence that TQ induces cancer cell death at least in part via inhibition of Akt phosphorylation leading DNA damage and activation of the mitochondrial-signaling proapoptotic pathway. Furthermore, TQ is also able to reduce the invasiveness of cancer cells and to sensitize LNM35 cancer cells to the cytotoxic effects of the DNA-damaging agent cisplatin. We also report an anticancer effect of TQ in a highly aggressive human lung cancer xenograft in nude mice. Recent study presented preliminary evidence for novel synthetic TQ analogs with biological activity that is better than the parental TQ without systemic toxicity [39]. In view of the available experimental findings, we contend that thymoquinone and /or its analogues may have a strong clinical potential as an anticancer drug either alone or in combination with some chemotherapeutic agents such as cisplatin.

ACKNOWLEDGEMENTS

This work was financially supported by the Research Affairs at the UAE University under a contract no. 02-04-8-11/07 and by Terry Fox Fund for Cancer Research to samir Attoub and haider Raza. The authors wish to thank Ms. Anne John and Ms. Manjusha Sudhadevi, Dept. of Pathology, Ms. Annie John, Dept. of Biochemistry FMHS for their excellent technical help. We thank Prof. Joan Massague from Howard Hughes Medical Institute for providing the MDA-MB-231 and MDA-MB-231-1833 cells and Dr. Mien-Chie Hung from University of Texas MD Anderson Cancer Center for providing the MDA-MB-435 cells.

REFERENCES

1 Parkin D.M., Bray F., Ferlay J., Pisani P. Global cancer statistics, 2002. CA Cancer J. Clin. (2005) **55** 74–108.
2 Gali-Muhtasib H., Roessner A., Schneider-Stock R. Thymoquinone: a promising anti-cancer drug from natural sources. Int. J. Biochem. Cell Biol. (2006) **38** 1249–1253.
3 Woo C.C., Kumar A.P., Sethi G., Tan K.H. Thymoquinone: potential cure for inflammatory disorders and cancer. Biochem. Pharmacol. (2011) **83** 443–451.
4 Gali-Muhtasib H., Diab-Assaf M., Boltze C., et al. Thymoquinone extracted from black seed triggers apoptotic cell death in human colorectal cancer cells via a p53-dependent mechanism. Int. J. Oncol. (2004) **25** 857–866.
5 Rooney S., Ryan M.F. Effects of alpha-hederin and thymoquinone, constituents of *Nigella sativa*, on human cancer cell lines. Anticancer Res. (2005) **25** 2199–2204.
6 Gurung R.L., Lim S.N., Khaw A.K., Soon J.F., Shenoy K., Mohamed Ali S. et al. Thymoquinone induces telomere shortening, DNA damage and apoptosis in human glioblastoma cells. PLoS ONE (2010) **5** e12124.
7 Kozaki K., Miyaishi O., Tsukamoto T., Tatematsu Y., Hida T., Takahashi T. Establishment and characterization of a human lung cancer cell line NCI-H460-LNM35 with consistent lymphogenous metastasis via both subcutaneous and orthotopic propagation. Cancer Res. (2000) **60** 2535–2540.
8 Raza H., Prabu S.K., Robin M.A., Avadhani N.G. Elevated mitochondrial cytochrome P450 2E1 and glutathione S-transferase A4-4 in streptozotocin-induced diabetic rats: tissue-specific variations and roles in oxidative stress. Diabetes (2004) **53** 185–194.
9 Raza H., John A. 4-hydroxynonenal induces mitochondrial oxidative stress, apoptosis and expression of glutathione S-transferase A4-4 and cytochrome P450 2E1 in PC12 cells. Toxicol. Appl. Pharmacol. (2006) **216** 309–318.
10 Li H., Gao Z., Kang L., Zhang H., Yang K., Yu K. et al. TarFisDock: a web server for identifying drug targets with docking approach. Nucleic Acids Res. (2006) **34** W219–W224.
11 Gao Z., Li H., Zhang H., Liu X., Kang L., Luo X. et al. PDTD: a web-accessible protein database for drug target identification. BMC Bioinformatics (2008) **9** 104.

12 Sethi G., Ahn K.S., Aggarwal B.B. Targeting nuclear factor-kappa B activation pathway by thymoquinone: role in suppression of antiapoptotic gene products and enhancement of apoptosis. Mol. Cancer Res. (2008) **6** 1059–1070.
13 Worthen D.R., Ghosheh O.A., Crooks P.A. The in vitro anti-tumor activity of some crude and purified components of blackseed, *Nigella sativa* L. Anticancer Res. (1998) **18** 1527–1532.
14 Shoieb A.M., Elgayyar M., Dudrick P.S., Bell J.L., Tithof P.K. In vitro inhibition of growth and induction of apoptosis in cancer cell lines by thymoquinone. Int. J. Oncol. (2003) **22** 107–113.
15 El-Mahdy M.A., Zhu Q., Wang Q.E., Wani G., Wani A.A. Thymoquinone induces apoptosis through activation of caspase-8 and mitochondrial events in p53-null myeloblastic leukemia HL-60 cells. Int. J. Cancer (2005) **117** 409–417.
16 Banerjee S., Kaseb A.O., Wang Z., Kong D., Mohammad M., Padhye S. et al. Antitumor activity of gemcitabine and oxaliplatin is augmented by thymoquinone in pancreatic cancer. Cancer Res. (2009) **69** 5575–5583.
17 Yi T., Cho S.G., Yi Z., Pang X., Rodriguez M., Wang Y. et al. Thymoquinone inhibits tumor angiogenesis and tumor growth through suppressing AKT and extracellular signal-regulated kinase signaling pathways. Mol. Cancer Ther. (2008) **7** 1789–1796.
18 Li F., Rajendran P., Sethi G. Thymoquinone inhibits proliferation, induces apoptosis and chemosensitizes human multiple myeloma cells through suppression of signal transducer and activator of transcription 3 activation pathway. Br. J. Pharmacol. (2010) **161** 541–554.
19 Arafa e.-S., Zhu Q., Shah Z.I., Wani G., Barakat B.M., Racoma I. et al. Thymoquinone up-regulates PTEN expression and induces apoptosis in doxorubicin-resistant human breast cancer cells. Mutat. Res. (2011) **706** 28–35.
20 El-Najjar N., Chatila M., Moukadem H., Vuorela H., Ocker M., Gandesiri M. et al. Reactive oxygen species mediate thymoquinone-induced apoptosis and activate ERK and JNK signaling. Apoptosis (2010) **15** 183–195.
21 Xu N., Hegarat N., Black E.J., Scott M.T., Hochegger H., Gillespie D.A. Akt/PKB suppresses DNA damage processing and checkpoint activation in late G2. J. Cell Biol. (2010) **190** 297–305.
22 Gali-Muhtasib H., Kuester D., Mawrin C., Bajbouj K., Diestel A., Ocker M. et al. Thymoquinone triggers inactivation of the stress response pathway sensor CHEK1 and contributes to apoptosis in colorectal cancer cells. Cancer Res. (2008) **68** 5609–5618.
23 Fesik S.W. Promoting apoptosis as a strategy for cancer drug discovery. Nat. Rev. Cancer (2005) **5** 876–885.
24 Rooney S., Ryan M.F. Modes of action of alpha-hederin and thymoquinone, active constituents of *Nigella sativa*, against HEp-2 cancer cells. Anticancer Res. (2005) **25** 4255–4259.
25 Wesierska-Gadek J., Gueorguieva M., Wojciechowski J., Tudzarova-Trajkovska S. In vivo activated caspase-3 cleaves PARP-1 in rat liver after administration of the hepatocarcinogen N-nitrosomorpholine (NNM) generating the 85 kDa fragment. J. Cell. Biochem. (2004) **93** 774–787.
26 Woo C.C., Loo S.Y., Gee V., Yap C.W., Sethi G., Kumar A.P. et al. Anticancer activity of thymoquinone in breast cancer cells: possible involvement of PPAR-γ pathway. Biochem. Pharmacol. (2011) **82** 464–475.
27 Kolli-Bouhafs K., Boukhari A., Abusnina A., Velot E., Gies J.P., Lugnier C. et al. Thymoquinone reduces migration and invasion of human glioblastoma cells associated with FAK, MMP-2 and MMP-9 down-regulation. Invest. New Drugs (2011).
28 Gali-Muhtasib H., Ocker M., Kuester D., Krueger S., El-Hajj Z., Diestel A. et al. Thymoquinone reduces mouse colon tumor cell invasion and inhibits tumor growth in murine colon cancer models. J. Cell Mol. Med. (2008) **12** 330–342.
29 Al-Ali A., Alkhawajah A.A., Randhawa M.A., Shaikh N.A. Oral and intraperitoneal LD50 of thymoquinone, an active principle of *Nigella sativa*, in mice and rats. J. Ayub Med. Coll. Abbottabad (2008) **20** 25–27.
30 Al-Amri A.M., Bamosa A.O. Phase I safety and clinical activity study of thymoquinone in patients with advanced refractory malignant disease. Shiraz E-Med. J. (2009) **10** 107–111.
31 Jafri S.H., Glass J., Shi R., Zhang S., Prince M., Kleiner-Hancock H. Thymoquinone and cisplatin as a therapeutic combination in lung cancer: in vitro and in vivo. J. Exp. Clin. Cancer Res. (2010) **29** 87.
32 Kaseb A.O., Chinnakannu K., Chen D., Sivanandam A., Tejwani S., Menon M. et al. Androgen receptor and E2F-1 targeted thymoquinone therapy for hormone-refractory prostate cancer. Cancer Res. (2007) **67** 7782–7788.
33 Badary O.A., Nagi M.N., al-Shabanah O.A., al-Sawaf H.A., al-Sohaibani M.O., al-Bekairi A.M. Thymoquinone ameliorates the nephrotoxicity induced by cisplatin in rodents and potentiates its antitumor activity. Can. J. Physiol. Pharmacol. (1997) **75** 1356–1361.
34 Nagi M.N., Mansour M.A. Protective effect of thymoquinone against doxorubicin-induced cardiotoxicity in rats: a possible mechanism of protection. Pharmacol. Res. (2000) **41** 283–289.
35 Ferraldeschi R., Baka S., Jyoti B., Faivre-Finn C., Thatcher N., Lorigan P. Modern management of small-cell lung cancer. Drugs (2007) **67** 2135–2152.
36 Lally B.E., Urbanic J.J., Blackstock A.W., Miller A.A., Perry M.C. Small cell lung cancer: have we made any progress over the last 25 years? Oncologist (2007) **12** 1096–1104.
37 Chehl N., Chipitsyna G., Gong Q., Yeo C.J., Arafat H.A. Anti-inflammatory effects of the *Nigella sativa* seed extract, thymoquinone, in pancreatic cancer cells. HPB (Oxford) (2009) **11** 373–381.
38 Hoeft B., Linseisen J., Beckmann L., Müller-Decker K., Canzian F., Hüsing A. et al. Polymorphisms in fatty-acid-metabolism-related genes are associated with colorectal cancer risk. Carcinogenesis (2010) **31** 466–472.
39 Banerjee S., Azmi A.S., Padhye S., Singh M.W., Baruah J.B., Philip P.A. et al. Structure-activity studies on therapeutic potential of Thymoquinone analogs in pancreatic cancer. Pharm. Res. (2010) **27** 1146–1158.

Frondoside A Suppressive Effects on Lung Cancer Survival, Tumor Growth, Angiogenesis, Invasion, and Metastasis

Samir Attoub[1]*, Kholoud Arafat[1], An Gélaude[2], Mahmood Ahmed Al Sultan[1], Marc Bracke[2], Peter Collin[3], Takashi Takahashi[4], Thomas E. Adrian[5], Olivier De Wever[2]

1 Department of Pharmacology & Therapeutics, Faculty of Medicine & Health Sciences, U. A. E. University, Al-Ain, United Arab Emirates, **2** Laboratory of Experimental Cancer Research, University Hospital, Gent, Belgium, **3** Coastside Bio Resources, Stonington, Maine, United States of America, **4** Division of Molecular Carcinogenesis, Center for Neurological Diseases and Cancer, Nagoya University Graduate School of Medicine, Nagoya, Japan, **5** Department of Physiology, Faculty of Medicine & Health Sciences, U. A. E. University, Al-Ain, United Arab Emirates

Abstract

A major challenge for oncologists and pharmacologists is to develop less toxic drugs that will improve the survival of lung cancer patients. Frondoside A is a triterpenoid glycoside isolated from the sea cucumber, *Cucumaria frondosa* and was shown to be a highly safe compound. We investigated the impact of Frondoside A on survival, migration and invasion *in vitro*, and on tumor growth, metastasis and angiogenesis *in vivo* alone and in combination with cisplatin. Frondoside A caused concentration-dependent reduction in viability of LNM35, A549, NCI-H460-Luc2, MDA-MB-435, MCF-7, and HepG2 over 24 hours through a caspase 3/7-dependent cell death pathway. The IC50 concentrations (producing half-maximal inhibition) at 24 h were between 1.7 and 2.5 μM of Frondoside A. In addition, Frondoside A induced a time- and concentration-dependent inhibition of cell migration, invasion and angiogenesis *in vitro*. Frondoside A (0.01 and 1 mg/kg/day i.p. for 25 days) significantly decreased the growth, the angiogenesis and lymph node metastasis of LNM35 tumor xenografts in athymic mice, without obvious toxic side-effects. Frondoside A (0.1–0.5 μM) also significantly prevented basal and bFGF induced angiogenesis in the CAM angiogenesis assay. Moreover, Frondoside A enhanced the inhibition of lung tumor growth induced by the chemotherapeutic agent cisplatin. These findings identify Frondoside A as a promising novel therapeutic agent for lung cancer.

Citation: Attoub S, Arafat K, Gélaude A, Al Sultan MA, Bracke M, et al. (2013) Frondoside A Suppressive Effects on Lung Cancer Survival, Tumor Growth, Angiogenesis, Invasion, and Metastasis. PLoS ONE 8(1): e53087. doi:10.1371/journal.pone.0053087

Editor: Srikumar P. Chellappan, H. Lee Moffitt Cancer Center & Research Institute, United States of America

Received June 13, 2012; **Accepted** November 27, 2012; **Published** January 8, 2013

Funding: This work was financially supported by the FMHS grant number NP/08/27 (SA), the UAE University grant under a contract no. 01-04-8-11/09 (SA), the Terry Fox Fund for Cancer Research (SA and TA), the UAEU-NRF 09/10 grant number 21MO72 (SA), and the Maine Technology Institute, Gardiner, Maine, USA, and the National Cancer Institute, RAPID Program (PC). The funding agencies had no role in study design, data collection and analysis, decision to publish, or preparation of the manuscript.

Competing Interests: Peter Collin is director, laboratory manager, employee and stock-holder of Coastside Bio Resources, a Maine, USA Corporation. Thomas Adrian and Peter Collin are co-inventors of a United States patent describing Frondoside A and other sea cucumber glycosides as putative anti-cancer agents, and may benefit financially if Frondoside A becomes a drug for human cancers. This does not alter the authors' adherence to all the PLOS ONE policies on sharing data and materials.

* E-mail: samir.attoub@uaeu.ac.ae

Introduction

Lung cancer is the most common form of cancer with one of the highest mortality rates in the world. Targeted therapies for selected subgroups of patients constitute a remarkable progress in the treatment of lung cancer. However, despite these advances, controversies remain, patients die, and a cure remains elusive [1]. Natural compounds are emerging as a new generation of anticancer agents with limited toxicity in cancer patients [2,3]. They can have high value in tumors resistant to classical chemotherapies or resistant to tyrosine kinase inhibitors such as gefitinib

Sea cucumbers have been valued for hundreds of years in the Chinese diet as a food delicacy, as well as a medicine for a wide variety of diseases. In the United States and Canada, sea cucumber tissues are dried, pulverized and encapsulated as nutraceuticals for over-the-counter dietary health supplements, primarily directed at inflammatory conditions in humans and companion animals [4]. Frondoside A is a triterpenoid glycoside isolated from the Atlantic cucumber, *Cucumaria frondosa*. (See [5] for chemical structure). Recent studies demonstrate that low concentrations of Frondoside A inhibit the growth and induced apoptosis of human pancreatic, leukemia and breast cancer cells via caspase activation [6–8].

The chemotherapeutic agents currently in use for lung cancer are still unsatisfactory due to associated co-lateral toxicity and drug-induced resistance [9–11] which motivate our investigation of the impact of Frondoside A on human non-small cell lung cancer survival, migration and invasion *in vitro*, and on tumor growth, metastasis and angiogenesis *in vivo* alone and in combination with cisplatin.